

FoxM1 Induced Paclitaxel Resistance via Activation of the FoxM1/PHB1/RAF-MEK-ERK Pathway and Enhancement of the ABCA2 Transporter

Chao Huang,¹ Xin Zhang,² Li Jiang,³ Limin Zhang,⁴ Ming Xiang,¹ and Hongyu Ren⁵

¹Department of Pharmacology, School of Pharmacy, Tongji Medical College, Huazhong University of Science and Technology, Wuhan 430030, China; ²Hepatic Surgery Center, Tongji Hospital, Tongji Medical College, Huazhong University of Science and Technology, Wuhan 430030, China; ³Department of Biliary and Pancreatic Surgery, Tongji Hospital, Tongji Medical College, Huazhong University of Science and Technology, Wuhan 430030, China; ⁴Institute of Organ Transplantation, Tongji Hospital, Tongji Medical College, Huazhong University of Science and Technology, Wuhan 430030, China; ⁵Division of Gastroenterology, Union Hospital, Tongji Medical College, Huazhong University of Science and Technology, Wuhan 430022, China

FoxM1 amplification in human pancreatic cancer predicts poor prognosis and resistance to paclitaxel. Here, a novel role between FoxM1 (FoxM1b and FoxM1c) and Prohibitin1 (PHB1) in paclitaxel resistance has been identified. We adopted a bioinformatics approach to predict the potential effector of FoxM1. It specifically bound to the promoter of PHB1, and it enhanced PHB1 expression at transcriptional and post-transcriptional levels. FoxM1 contributed to the PHB1/C-RAF interaction and phosphorylation of ERK1/2 kinases, thus promoting paclitaxel resistance. Notably, FoxM1 conferred tumor cell resistance to paclitaxel, but knocking down PHB1 could sensitize pancreatic cancer cells to it. Besides, we identified that ABCA2 promoted paclitaxel resistance under the regulation of FoxM1/PHB1/RAF-MEK-ERK. Thiostrepton, an inhibitor of FoxM1, significantly decreased the expression of PHB1, p-ERK1/2, and ABCA2. It increased the influx of paclitaxel into the cell, and it attenuated FoxM1-mediated paclitaxel resistance *in vitro* and *in vivo*. Collectively, our findings defined PHB1 as an important downstream effector of FoxM1. It was regulated by FoxM1 to maintain phosphorylation of ERK1/2 in drug-resistant cells, and FoxM1 simultaneously enhanced the function of ABCA2, which collectively contributed to paclitaxel resistance. Targeting FoxM1 and its downstream effector PHB1 increased the sensitivity of pancreatic cells to paclitaxel treatment, providing potential therapeutic strategies for patients with paclitaxel resistance.

INTRODUCTION

Pancreatic cancer always has poor prognosis with survival rate of less than 5%. Standard therapy for advanced pancreatic adenocarcinoma is combined chemotherapy, mostly gemcitabine and paclitaxel. However, the common challenges for chemotherapy, such as multidrug resistance and high toxicity, also limit the use of paclitaxel. Many attempts have been made to find useful markers of paclitaxel resistance and develop strategies to reverse paclitaxel resistance, but the results are not so satisfactory.¹

Drug resistance is a multifactorial process including a series of modifications. In the case of paclitaxel, several potential mechanisms have been proposed to account for the resistance observed in human tumors and cancer cell lines. These include overexpression of the multidrug ATP-binding cassette (ABC) transporters² and alterations in the dynamics of microtubules and tubulin.^{3,4} Besides, the extracellular signal-regulated kinase (ERK) that interacts with microtubules also contributes to paclitaxel resistance.⁵

FoxM1 is an oncogenic transcription factor of the Forkhead family. It has a well-defined role in the cell-cycle progression.⁶ Deregulation of FoxM1 is associated with poor prognosis in many types of human cancers, including pancreatic cancer, lung cancer, breast cancer, and so on.⁷⁻⁹ Moreover, cells overexpressing FoxM1 are resistant to apoptosis or premature senescence induced by oxidative stress,⁶ which has strong implications for resistance to chemotherapy. It is noteworthy that breast cancer cells with the overexpression of FoxM1 show resistance to cisplatin, trastuzumab, and paclitaxel.¹⁰ Growth factors activate receptors to initiate signaling pathways, such as PI3K-AKT and MAPK. Aberrant activation of RAS, RAF, or MAPK in tumor cells leads to ERK1/2-mediated phosphorylation and nuclear accumulation of FoxM1, which promotes the FoxM1-dependent transcriptional activity.¹¹

Rajalingam et al.¹² reported that Prohibitin1 (PHB1) acted as an important signaling scaffold at the plasma membrane, where it was necessary for the recruitment of C-RAF to Caveolin-1-rich lipid rafts and the activation of the RAS-RAF-MEK-ERK pathway. Clinical and mechanistic evidence supported the novelty of the FoxM1-Caveolin-1 (Cav-1)-signaling pathway and its indispensable contribution to pancreatic cancer invasion and metastasis.¹³ PHB1 and Caveolin-1

Received 13 February 2019; accepted 7 May 2019;
<https://doi.org/10.1016/j.omto.2019.05.005>.

Correspondence: Hongyu Ren, Division of Gastroenterology, Union Hospital, Tongji Medical College, Huazhong University of Science and Technology, Wuhan 430022, China.

E-mail: hongyur@hotmail.com



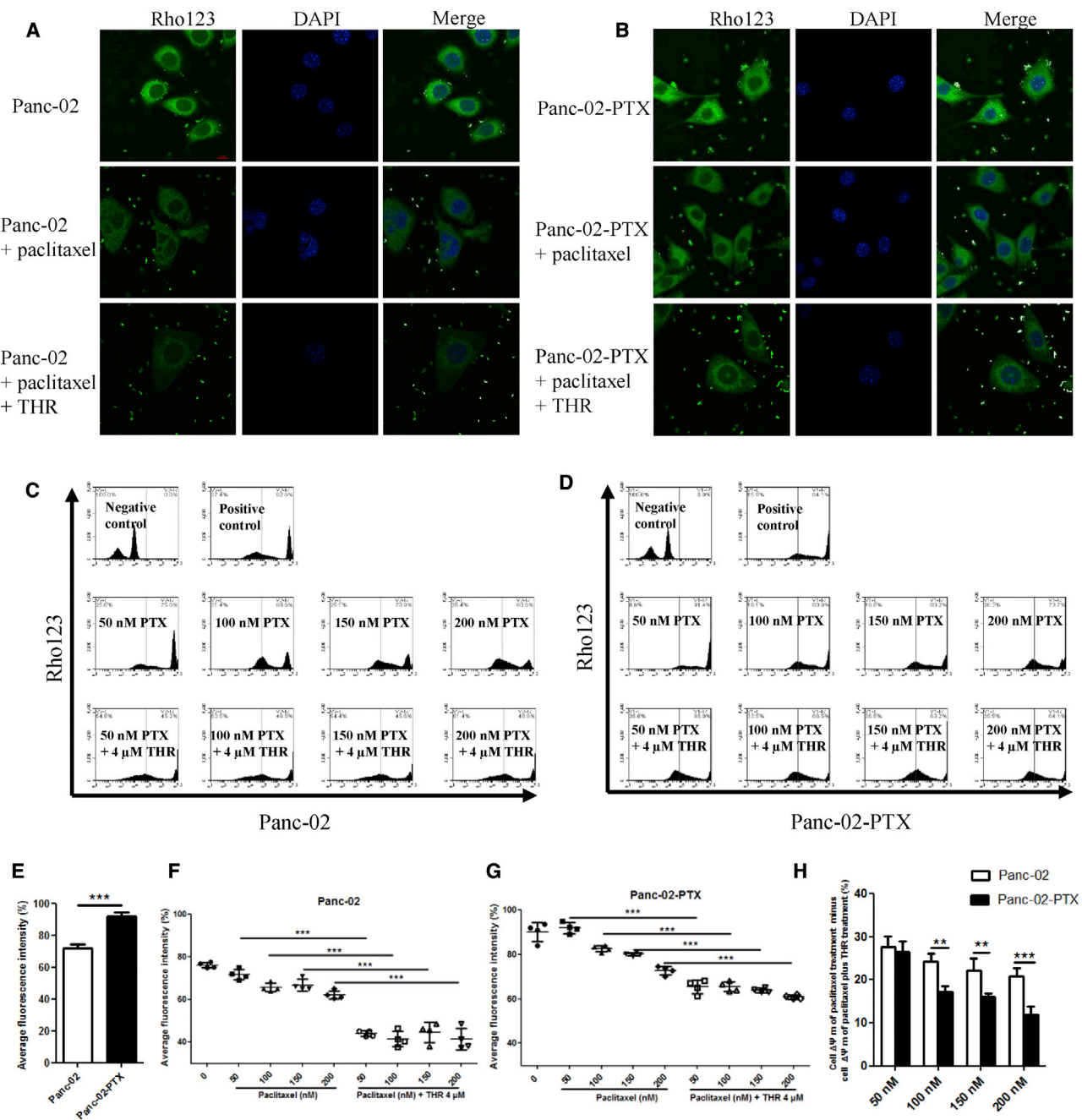


Figure 1. THR Significantly Reduced Mitochondrial Membrane Potential of Pancreatic Cancer Cells

(A and B) Representative confocal images of Panc-02 (A) and Panc-02-PTX (B) cell lines treated with DMSO, paclitaxel (100 nM), and paclitaxel (100 nM) and THR (4 μM), respectively, for 24 h and then stained with Rho123 (green) and DAPI (blue). Scale bar, 10 μm. (C and D) 10,000 Panc-02 (C) and Panc-02-PTX (D) cells were used in the flow cytometric analysis. After 24-h treatment, Rho123 (5 μg/mL) was added to the cell culture. Cells untreated and treated with Rho123 were used as negative and positive controls, respectively. The first line represents the negative and positive controls of the experiment. The second line represents Panc-02 or Panc-02-PTX, which was incubated with paclitaxel at the concentrations of 50, 100, 150, and 200 nM, respectively. The third line represents the Panc-02 or Panc-02-PTX, which was incubated with paclitaxel at the concentrations of 50, 100, 150, and 200 nM and combined with THR (4 μM), respectively. (E) Quantification of the mitochondrial membrane potential ($\Delta\Psi_m$) of Panc-02 and Panc-02-PTX. Data were represented as means \pm SD. Statistical significance was calculated with unpaired Student's t test. $n = 4$, $***p < 0.001$. (F and G) Quantification of the $\Delta\Psi_m$ of Panc-02 (F) or Panc-02-PTX (G) treated with DMSO, paclitaxel, and paclitaxel

(legend continued on next page)

are two different types of lipid rafts (planar rafts and caveolae). The distinguishing factor is that the caveolae are formed by the protein caveolin, whereas the planar rafts lack this protein.¹⁴ Flotillin and epidermal surface antigen define a new family of caveolae-associated integral membrane proteins.¹⁵ The structure of mammalian Stomatin/Prohibitin/Flotillin/HflK/C (SPFH) domain-containing proteins include prohibitin-1 and prohibitin-2, erlin-1 and erlin-2, podocin, stomatin-1, and flotillin-1 and flotillin-2, which indicates that PHB1 and Caveolin-1 share the SPFH domain. Therefore, we investigated the molecular mechanisms of FoxM1 and PHB1 in paclitaxel resistance in pancreatic cancer.

PHB1 is an evolutionarily conserved 32-kDa protein that is multifunctional in cellular biology, including as a molecular chaperone and in cellular proliferation, cellular apoptosis, and mitochondrial energy metabolism.^{16,17} PHB1 is essential for the stabilization of mitochondrial integrity and membrane potential in human ovarian cancer cells.^{18,19} Overexpression of PHB1 conferred cell resistance to staurosporine via the intrinsic apoptotic pathway. In contrast, silencing of PHB1 expression sensitized ovarian cancer cells to staurosporine.¹⁸ We found that paclitaxel-resistant cells harbored higher mitochondrial properties than the sensitive ones, as indicated by Rhodamine 123 (Rho123), a probe of the mitochondrial membrane potential.²⁰ Similarly, FoxM1 inhibitor thioestrepton (THR) decreased the Rho123 retention in the paclitaxel-resistant and -sensitive cells, and this phenomenon was excluded from the function of P-glycoprotein (P-gp or ABCB1) by detecting the cross-resistance to doxorubicin (DOX). Therefore, we speculated that FoxM1 might contribute to the development of paclitaxel resistance via regulating PHB1.

We determined the role of FoxM1 and PHB1 in pancreatic cancer and the mechanisms of paclitaxel resistance. The expression of FoxM1 and PHB1 correlated positively in pancreatic cancer cells and tumor tissues. FoxM1 bound to the promoter region of PHB1 and positively enhanced its transcriptional activity. Paclitaxel-resistant cell lines showed higher levels of FoxM1 and PHB1 compared with the sensitive ones. Overexpression of FoxM1 decreased the cellular apoptosis induced by paclitaxel in paclitaxel-sensitive cell lines, whereas knockdown of PHB1 at the same time could reverse this effect. On the other hand, after screening the gene expression of ABC transporters, we discovered that FoxM1 sustained the expression of ABCA2, at both the protein and mRNA levels, and decreased the intracellular concentrations of paclitaxel under the regulation of the FoxM1/PHB1/RAF-MEK-ERK feedback loop. In summary, FoxM1 regulated PHB1 expression, and it circulated the FoxM1/PHB1/RAF-MEK-ERK loop continuously to activate the expression of ABCA2, which conferred the cellular drug resistance.

RESULTS

FoxM1 Inhibitor THR Reduced Mitochondrial Membrane Potential of Paclitaxel-Resistant and -Sensitive Cell Lines

Paclitaxel-resistant cells Panc-02-PTX and A549-PTX had an elevated mitochondrial membrane potential, which was an indicator of hypersensitivity to Rhodamine 123 (Rho123). Zinkewich-Péotti and Andrews²¹ had addressed that the mitochondrial membrane potential was directly related to the cisplatin-resistant phenotype rather than a random alteration. The fluorescent intensity of Rho123 was higher in drug-resistant cell lines than in drug-sensitive cell lines, indicating that resistant cell lines were hypersensitive to Rho123 (Figures 1A–1E). Recently, it had been reported that ovarian cancer cell lines with higher membrane potentials were resistant to cisplatin, and this increase in membrane potential was not dependent on changes in the P-gp, the substrate of which was Rho123.^{21,22} Moreover, there was an inverse relationship between cisplatin and Rho123 resistance. It was similar to the paclitaxel and Rho123 (Figures S1H and S1I).

To eliminate the possibility that the THR-decreased retention of Rho123 was partially due to an increase in P-gp,²³ we tested the 4 cell lines for cross-resistance to DOX. Aspc-1, SW1990, Panc-02, and Panc-02-PTX had virtually identical IC₅₀ (half maximal [50%] inhibitory concentration) values of DOX (Figure S1D), which was consistent with the average intensity of DOX among the four cell lines after treatment with THR (Figures S1F and S1G). Flow cytometric analysis of cells stained with Rho123 showed clear differences between Panc-02-PTX and Panc-02. After the administration of THR, the membrane potentials of both sensitive and resistant cell lines were decreased (Figures 1F and 1G). Moreover, we found a more significant decrease in cell membrane potential in the Panc-02 cell line compared with the Panc-02-PTX cell line when treated with THR (Figure 1H). It was probably related to the expression level of FoxM1 between the two cell lines. The same results were obtained in A549-PTX and A549 cell lines (Figures S1A–S1C). We concluded that THR can decrease mitochondrial activity in paclitaxel-resistant or -sensitive cells. It increased the Rho123 resistance, which had an inverse relationship with paclitaxel resistance.

Close Relationship between the Expressions of FoxM1 and PHB1 in Pancreatic Cancer

Rho123 was a mitochondria-specific fluorescent dye. It was well known that PHB1 was isomorphic with the mitochondria and was highly expressed in cells. It showed a particular reliance on mitochondrial metabolism.²⁴ Could THR regulate the activity of mitochondria to mediate the paclitaxel resistance? We analyzed the data from GeneMANIA (<http://genemania.org/>), and we chose a gene expression database containing the expression profiles of FoxM1 and PHB1 in 218 tumor samples, which represented 14 kinds of common

and THR. One-way ANOVA post Tukey's multiple comparison test was used for statistical analysis. $n = 4$, $***p < 0.001$. (H) The $\Delta\Psi_m$ of Panc-02 cells treated with paclitaxel minus the $\Delta\Psi_m$ of Panc-02 treated with the same dosage of paclitaxel and THR (4 μM), respectively. The $\Delta\Psi_m$ of Panc-02-PTX cells treated with paclitaxel minus the $\Delta\Psi_m$ of Panc-02-PTX cells treated with the same dosage of paclitaxel and THR (4 μM), respectively, is also shown. Statistical analysis was performed by Student's *t* test. $**p < 0.01$, $***p < 0.001$.

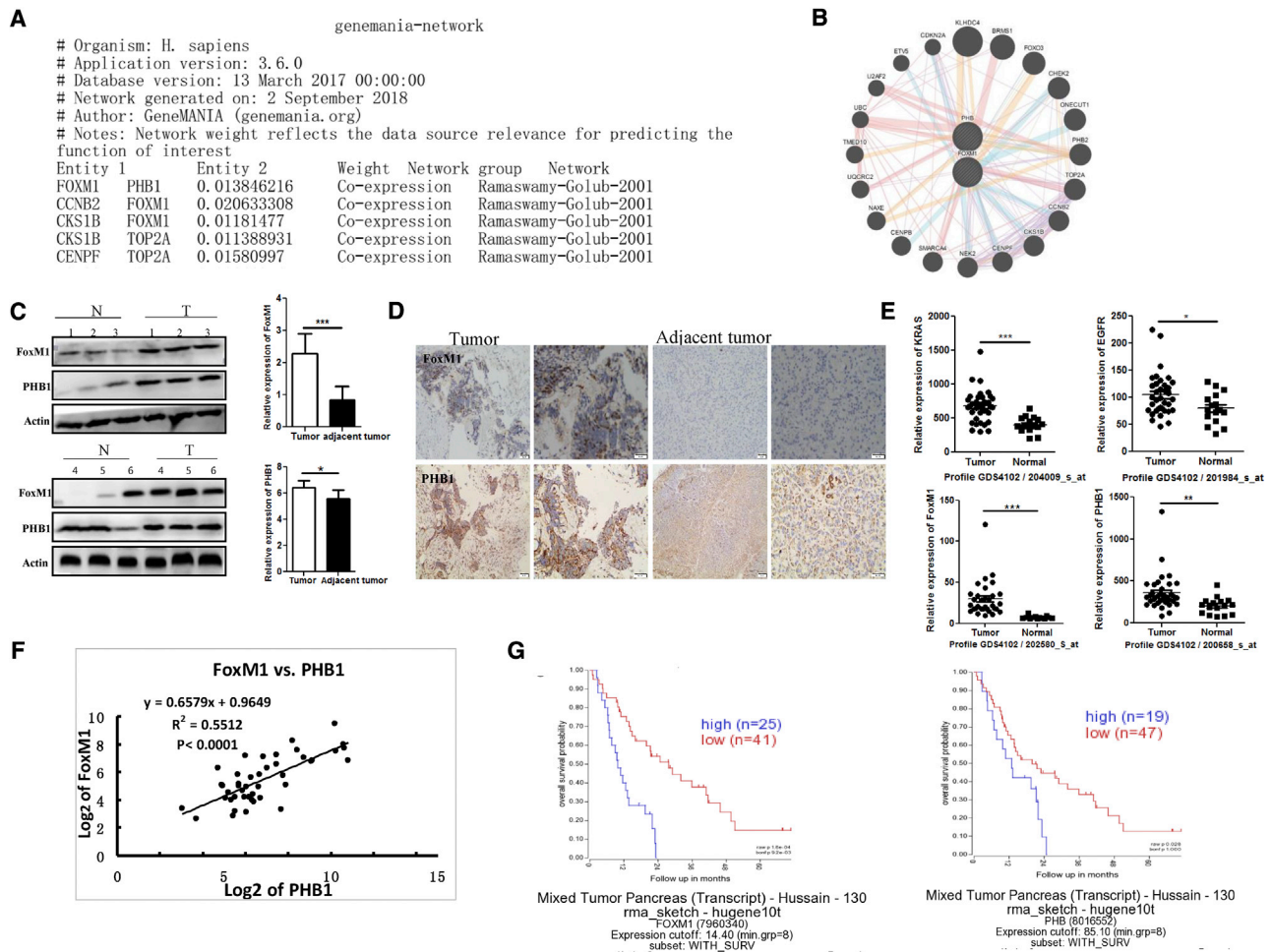


Figure 2. FoxM1 and PHB1 Were Highly Expressed in Pancreatic Cancer and Closely Correlated

(A) The pattern of correlations between FoxM1 and PHB1 was stored by the GeneMANIA network. FoxM1 and PHB1 were co-expressed and clustered in the database from Ramaswamy et al.²⁵ (B) Genes associated with FoxM1 and PHB1 were represented by circles. Networks were divided into 7 parts. Physical interaction among them was 67.64%, co-expression was 13.50%, predicted was 6.35%, co-localization was 6.17%, pathway was 4.35%, gene interaction was 1.40%, and shared gene domain was 0.59%. (C and D) Western blot (C) and IHC (D) protein expressions were detected in adjacent normal tissue and pancreatic cancer tissue. The expressions of FoxM1 and PHB1 in the adjacent normal pancreatic tissue were lower than those of the pancreatic cancer tissue. Scale bars, 50 and 100 μ m, respectively. (E) GEO: GSE16515 data indicated that the upstream stimulation signals KRAS and EGFR were higher expressed in the tumor compared with the adjacent normal tissue, which was similar to FoxM1 and PHB1. (F) The mRNA levels of FoxM1 and PHB1 from the GEO data were positively correlated. $r = 0.7424$, $p < 0.0001$. (G) Kaplan-Meier survival curve of patients was conducted based on the expressions of FoxM1 and PHB1. Data were generated from the dataset (Tumor Pancreatic ductal adenocarcinoma-Yeh-132-custom-4hm44k; <https://hgserver1.amc.nl/cgi-bin/r2/main.cgi>). * $p < 0.05$, ** $p < 0.01$, *** $p < 0.001$.

human cancers.²⁵ FoxM1 and PHB1 had been clustered in the database (Figure 2A). The gene network and interactions file between FoxM1 and PHB1 is in Figure 2B and Table S3. The expressions of FoxM1 and PHB1 in pancreatic cancer tissues were detected by western blot (WB) and immunohistochemistry (IHC) (Figures 2C and 2D), and their direct correlation was found statistically significant in the database ($r = 0.742$; $p < 0.001$; Figure 2F). GEO: GSE16515²⁶ showed that KRAS, EGFR, FoxM1, and PHB1 were highly expressed in pancreatic cancer tissue compared with normal tissue (Figure 2E). Kaplan-Meier survival curves showed that the overexpression of FoxM1 and PHB1 significantly associated with poorer survival in

pancreatic cancer patients (Figure 2G). Data were generated from the dataset accessible at <https://hgserver1.amc.nl/cgi-bin/r2/main.cgi>.

FoxM1 Promoted the Expression of PHB1

By using the FoxM1 consensus sequences 5'-A (C/T) AAA (C/T) AA-3',^{27,28} 5'-AGATTGAGTA-3',²⁹ and 5'-TAATCA-3',³⁰ we tried to find the potential FoxM1-binding elements in PHB1 promoter; 4 putative FoxM1-binding elements (referred to as DNA sequences 1-4) were identified. To provide direct proof that FoxM1b and FoxM1c were recruited to the endogenous PHB1 promoter during transcription, we conducted chromatin immunoprecipitation

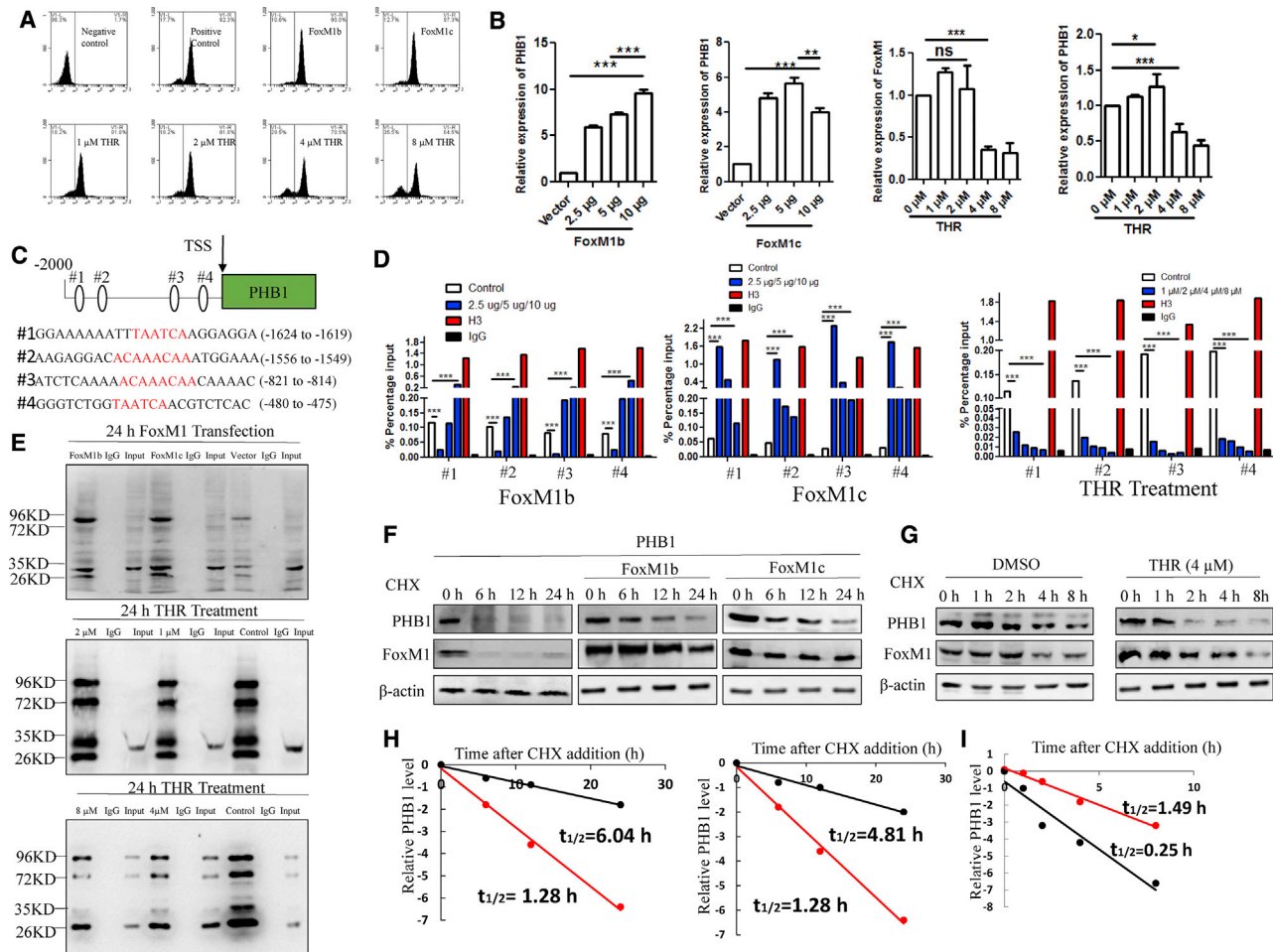


Figure 3. FoxM1 Regulated the Transcriptional and Post-transcriptional Activity of PHB1

(A) Fluorescence-activated cell sorting (FACS) was used to analyze the alterations of PHB1 protein after overexpression or suppression of FoxM1 in Bxpc-3. Cells were transfected with penter-FoxM1b or penter-FoxM1c or treated with 1, 2, 4, or 8 μ M THR for 24 h. Cells untreated or transfected with vector were used as negative and positive controls, respectively. (B) HEK293T cells were transiently transfected with penter-FoxM1b or penter-FoxM1c in a dose-dependent manner. The mRNA fold change of PHB1 was plotted relative to the vector. Dose-dependent suppression of FoxM1 by treating with THR at the dosages of 1, 2, 4, and 8 μ M was plotted relative to DMSO. Data were represented as means \pm SD. One-way ANOVA post Tukey's multiple comparison test was used for statistical analysis. * $p < 0.05$, ** $p < 0.01$, *** $p < 0.001$. (C) Sequences and positions of putative FoxM1-binding elements were plotted on the PHB1 promoter region (1–4). (D) ChIP assay. Chromatins were isolated from HEK293T cells. The enrichment percentage = $2\% \times 2^{CT[\text{Input sample}] - CT[\text{IP sample}]}$. HEK293T cells were transfected with the penter-FoxM1b or penter-FoxM1c at dosages of 2.5, 5, and 10 μ g. THR was at the concentrations of 1, 2, 4, and 8 μ M. Oligonucleotides flanked the PHB1 promoter regions that were containing putative FoxM1-binding sites, as given in Table S2. Normal IgG and Histone H3 were used as negative and positive controls, respectively. 2% of the total cell lysates was also subjected to immunoprecipitation (input sample). (E) Analyses of interactions between FoxM1 and PHB1 were detected in HEK293T cells. CoIP was performed in HEK293T cells transfected with penter-FoxM1b or penter-FoxM1c. PHB1 showed elevated binding activity compared with the input. Precipitation with the IgG was used as a negative control for the specificity of binding. (F) HEK293T cells were transfected with penter-PHB1 in the presence or absence of penter-FoxM1b and penter-FoxM1c, as indicated. 24 h later, cells were treated with cycloheximide (CHX, 50 μ g/mL) and harvested at the indicated time points. PHB1 and FoxM1 levels were analyzed by western blot. β -actin was used as a loading control. (G) HEK293T cells were subjected to DMSO or THR (4 μ M) for 24 h, then treated with cycloheximide (CHX, 50 μ g/mL) and harvested at the indicated time points. (H and I) Quantitation of the stability of PHB1. The PHB1 was detected after transfection with FoxM1 DNA (H) or FoxM1 inhibitor (I). PHB1 band density was normalized to β -actin and then normalized to $t = 0$ control; the red line represented the control group.

(ChIP) assays using chromatins prepared from HEK293T. The regions in the PHB1 promoter were flanked by 4 primers, including the 169-bp site 1 (–1,725 to –1,557), 139-bp site 2 (–1,618 to –1,480), 210-bp site 3 (–895 to –686), and 210-bp site 4 (–545 to –336). We observed detectable binding of FoxM1b and FoxM1c to sites 1–4 (Figure 3C).

Overexpression of the two isoforms of FoxM1 with increasing dose promoted the PHB1 transcriptional activity compared with the Histone H3 and immunoglobulin G (IgG) groups. But FoxM1b and FoxM1c exhibited different binding capacities. FoxM1b enhanced the enrichment of the four binding regions in a dose-dependent manner while FoxM1c did not (Figure 3D). It was consistent with

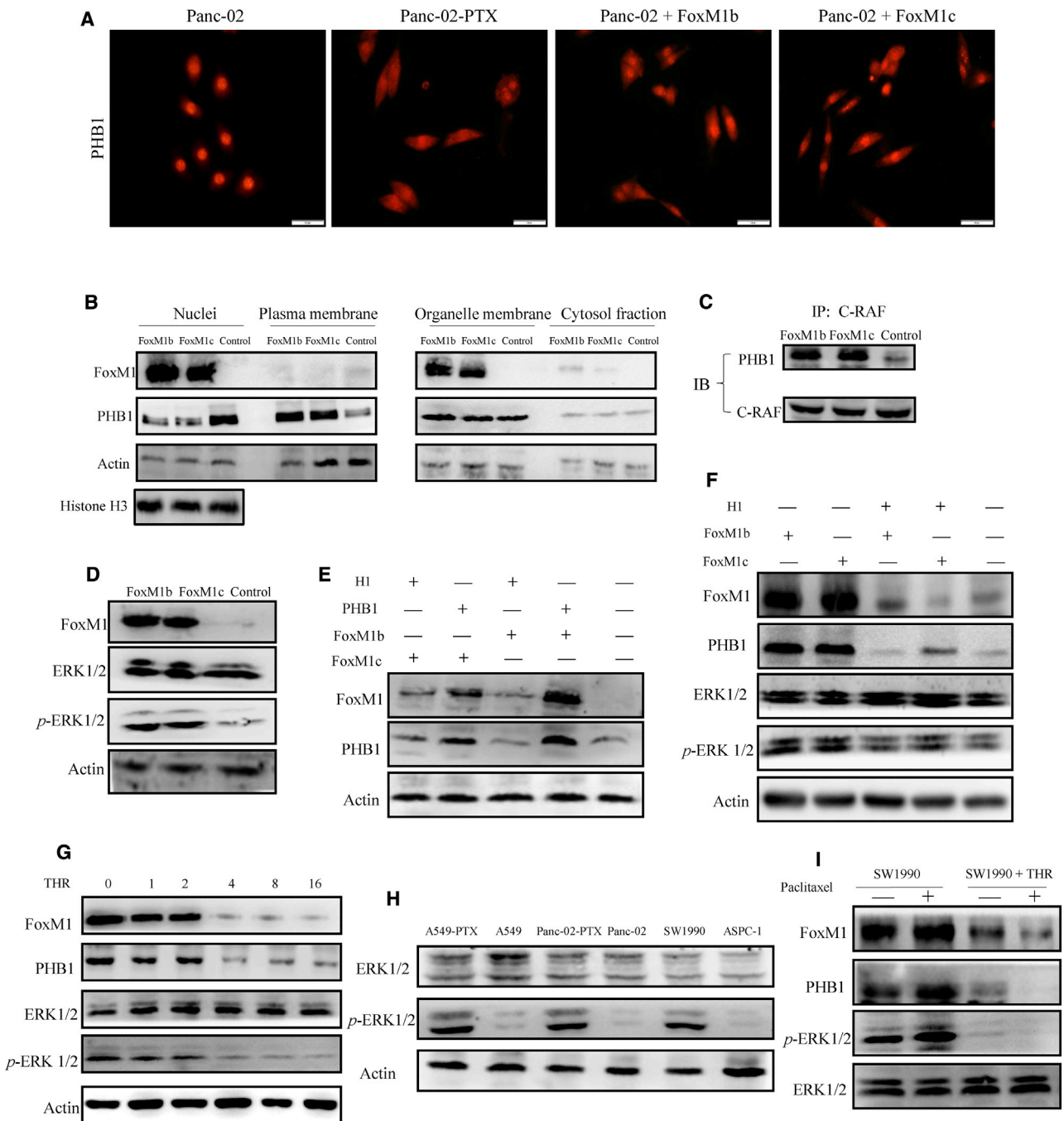


Figure 4. PHB1 Was Elevated on the Surface to Enhance the RAF-MEK-ERK Activity and Was Essential to the Activation of the FoxM1/PHB1/RAF-MEK-ERK Feedback Loop in Paclitaxel-Resistant Cells

(A) The distribution of PHB1 was detected in the Panc-02 or Panc-02-PTX. Panc-02 was transfected with penter-FoxM1b or penter-FoxM1c. Panc-02 or Panc-02-PTX was transfected with vector and stained for PHB1 with specific polyclonal antibody. Scale bar, 50 μ m. (B) To confirm the distribution of PHB1 in the pancreatic cells, Panc-02 cells were overexpressed with FoxM1b and FoxM1c. Fractions were separated from the nuclei, plasma membrane, organelle membrane, and cytosol fraction. Western blot showed the distribution of FoxM1 or PHB1 in the fractions. Actin and Histone H3 were used as loading controls. (C) Panc-02 cells were transfected with penter-FoxM1b and penter-FoxM1c for 24 h. Cell membrane lysates were co-immunoprecipitated with anti-C-RAF antibody. Immunoprecipitation complex was immunoblotted with PHB1 antibody. C-RAF was used as a loading control. (D) The Aspc-1 cells were transfected with penter-FoxM1b and penter-FoxM1c for 24 h. The whole-cell extracts were incubated with ERK1/2 and *p*-ERK1/2. (E and F) The Bxpc-3 cells were transfected with Plentiv2-PHB1 (H1) against FoxM1 overexpression for 24 h (E). Overexpression of

(legend continued on next page)

the mRNA level of PHB1, when it was transfected with the increasing dosage of FoxM1 (Figure 3B), and the protein level of Bxpc-3, when it was transfected with FoxM1b or FoxM1c or treated with the increasing dosage of THR 1 (Figure 3A). The natural splice variance of FoxM1b and FoxM1c may account for their different binding capacities.⁹ HEK293T cells treated with THR at concentrations of 4 and 8 μM depressed the FoxM1 and PHB1 levels, while the 1 and 2 μM could not. THR (1, 2, 4, and 8 μM) led to the decrease in FoxM1 recruitment to PHB1 promoter in HEK293T cells (Figure 3D). Collectively, our findings strongly supported that FoxM1 could transcriptionally activate PHB1 by interacting with four predicted binding sites.

To further examine the potential interaction between FoxM1 and PHB1, HEK293T cells were transfected with FoxM1b or FoxM1c and then subjected to immunoprecipitation (IP) analysis. Immunoblotting (IB) analysis revealed that PHB1 was present in anti-FoxM1 IP pellets (Figure 3E, top). When treated with THR at concentrations of 4 and 8 μM , it decreased the binding capability between FoxM1 and PHB1, while 1 and 2 μM could not (Figure 3E, middle and bottom). Moreover, coIP experiments were consistent with the results of ChIP-qPCR, flow cytometric, and qPCR detection (Figures 3A, 3B, and 3D). Our results suggested that PHB1 protein physically interacted with FoxM1 protein.

Next, we tried to understand how FoxM1 regulated PHB1 at a post-transcriptional level. Time course analysis revealed that exogenous overexpression of FoxM1b or FoxM1c significantly enhanced the half-life of PHB1 in HEK293T cells, from 1.49 to 6.04 and 4.81 h, respectively (Figures 3F and 3H). The opposite was observed with THR treatment: it significantly shortened the half-life of PHB1 from 1.28 to 0.25 h (Figures 3G and 3I), supporting that FoxM1 could regulate PHB1 through enhancing protein stability.

FoxM1/PHB1/RAF-MEK-ERK Integrated a Feedback Loop

We explored how FoxM1 regulated PHB1 in pancreatic cancer cells. The immunostaining results indicated that PHB1 was mainly distributed in the nucleus of the Panc-02 cells. Panc-02 transfected with FoxM1b or FoxM1c showed that PHB1 shifted from the nucleus to the cytoplasm membrane, which was consistent with the distribution of PHB1 in the Panc-02-PTX cells (Figure 4A). The Minute Plasma Membrane Protein Isolation and Cell Fractionation Kit (Invent, SM005) verified the immunostaining results. Panc-02 cell transfected with FoxM1b or FoxM1c showed that PHB1 was decreased in the nucleus and increased in the cytoplasm membrane (Figure 4B), which was consistent with the content of distribution in Panc-02 and Panc-02-PTX cells (Figure S4A).

Previously, a study had shown that PHB1 directly interacted with C-RAF via the C-terminal 32 amino acids.³¹ We detected a direct interaction of C-RAF and PHB1 *in vitro*. PHB1 in the membrane protein was pulled down by the C-RAF antibody and showed a significantly higher level than that of control when transfected with FoxM1b or FoxM1c in Panc-02 (Figure 4C). PHB1 participated in the phosphorylation of ERK1/2 induced by FoxM1. To evaluate the influence of FoxM1 on PHB1 expression, we overexpressed FoxM1b or FoxM1c in the Aspc-1 cell line, and we observed the increase in *p*-ERK1/2 (Figure 4D). Was the FoxM1-induced phosphorylation of ERK1/2 mediated by PHB1? We found that silencing PHB1 expression by transfecting Plentiv2-PHB1 (H1) plasmid strongly reduced the phosphorylation of ERK1/2 in SW1990 (Figure S3B) and overexpressing PHB1 could increase the *p*-ERK1/2 in Aspc-1 (Figure S3C). All the transfections were verified by qPCR (Figure S3A).

As previous researchers had revealed that FoxM1 was one of the effectors of ERK1/2,³² we speculated that FoxM1 regulated PHB1 to sustain ERK1/2 activity in a feedback circuit. Interestingly, we also found the corresponding changes of FoxM1, PHB1, and *p*-ERK1/2 when knocking down or overexpressing PHB1 (Figures 4E and 4F). Pharmacological suppression of FoxM1 by THR at the concentrations of 4, 8, and 16 μM led to a prominent decline in FoxM1, PHB1, and *p*-ERK1/2 protein abundance in the SW1990 cells, but it had no effect on total ERK1/2 level (Figure 4G). We analyzed the pancreatic cancer paclitaxel-resistant or -sensitive cell lines. The western blot showed that the level of *p*-ERK1/2 in drug-resistant cell lines was elevated when compared with that of drug-sensitive cell lines (Figure 4H). SW1990 cells treated with paclitaxel and THR significantly reduced the *p*-ERK1/2; ERK1/2 was a loading control (Figure 4I). We concluded that FoxM1 increased the phosphorylation of ERK1/2 via the FoxM1/PHB1/RAF-MEK-ERK feedback loop, which activated the genes involved in paclitaxel resistance.

FoxM1 and PHB1 Were Required for Paclitaxel Resistance of Pancreatic Cancer Cells and Non-Small-Cell Lung Cancer Cells

To determine the functional significance of the factors that were correlated in paclitaxel resistance, the protein and mRNA levels of PHB1 and FoxM1 were detected. PHB1 directly correlated with the expression pattern of FoxM1 in pancreatic cancer cells and non-small-cell lung cancer cells (Figures 5A and 5B). What is more, the relative mRNA levels of PHB1 in the 11 cell lines were positively correlated with their IC_{50} values (relative to paclitaxel), respectively (Figure 5C; Figure S1E). Western blot showed that the expression of PHB1 increased as expected when Aspc-1 was transfected with FoxM1b or FoxM1c (Figure 5D). Could FoxM1 influence the

FoxM1b or FoxM1c complemented PHB1 and *p*-ERK1/2 to the control level when it was co-transfected with the H1 plasmid (F). (G) The SW1990 cells were treated with THR *in vitro* at the dosages of 1, 2, 4, 8, and 16 μM . After 24 h, the expressions of FoxM1, PHB1, ERK1/2, and *p*-ERK1/2 were analyzed in the cell lysates. (H) Activation of *p*-ERK1/2 in paclitaxel-resistant and -sensitive cell lines was analyzed. ERK1/2 was used as a control. (I) Analysis of the expression level of *p*-ERK1/2 in SW1990 cells treated with paclitaxel (100 nM), THR (4 μM), and paclitaxel (100 nM) and THR (4 μM), respectively. ERK1/2 was used as a control.

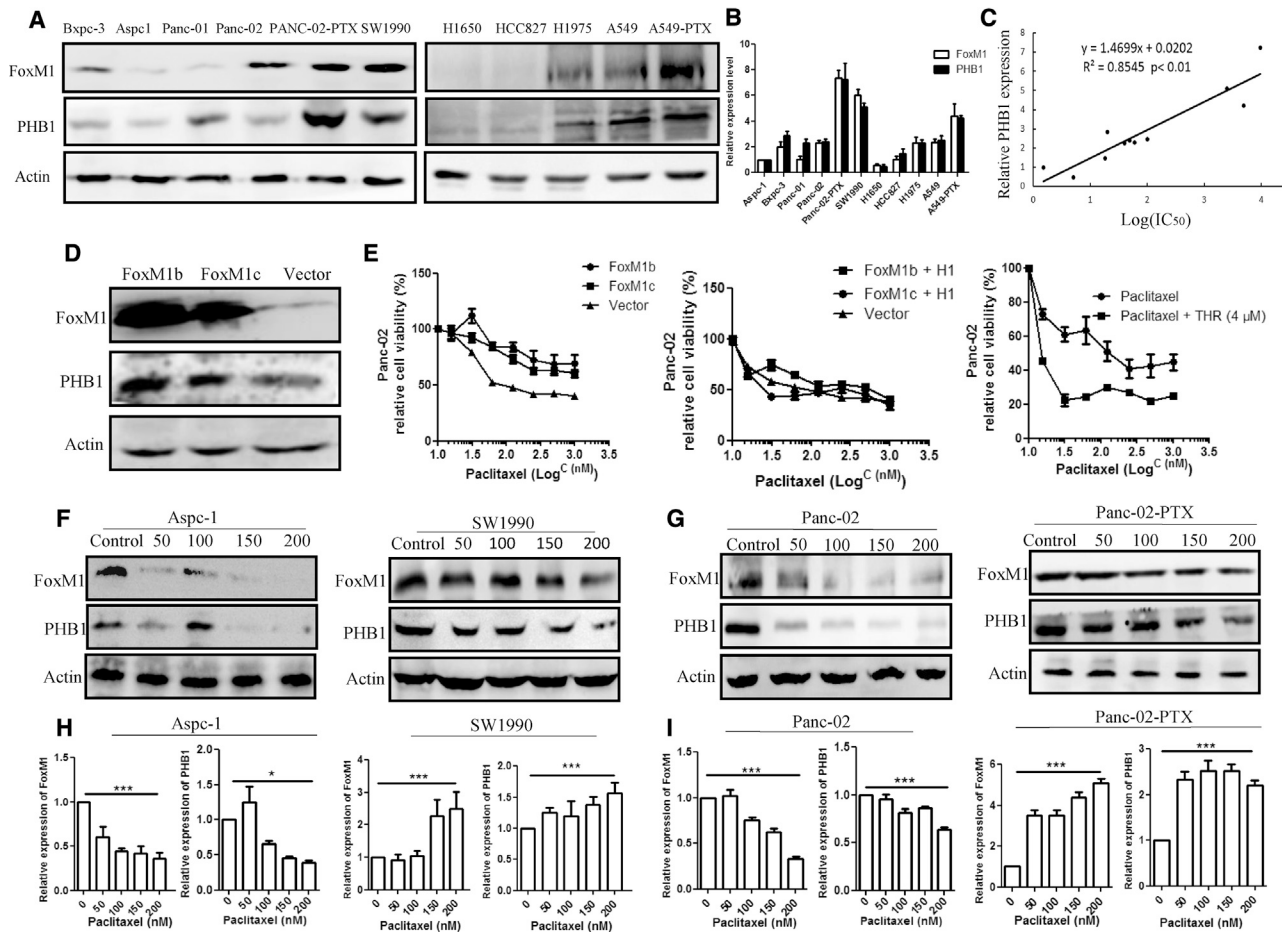


Figure 5. Higher Expressions of FoxM1 and PHB1 Contributed to Paclitaxel Drug Resistance

(A) Western blot analyzed the FoxM1 and PHB1 protein expression levels in pancreatic cancer cells and non-small-cell lung cancer cells. β -actin was used as a loading control. (B and C) The mRNA levels of FoxM1 and PHB1 were detected by qPCR (B) and PHB1 was positively correlated with the IC_{50} in the pancreatic cancer cells and non-small-cell lung cancer cells (C) ($r = 0.8653$, $p = 0.0407$). (D) Overexpression FoxM1b or FoxM1c induced PHB1 upregulation in Aspc-1. (E) Panc-02 was incubated with the varying concentrations of paclitaxel in a 96-well plate for 48 h; additionally, after it was transfected with penter-FoxM1b, penter-FoxM1c, co-transfected with penter-FoxM1b and H1, and co-transfected with penter-FoxM1c and H1 for 24 h. MTT (3-(4,5-dimethyl-2-thiazolyl)-2,5-diphenyl-2-H-tetrazolium bromide) assay was used to assess the cell viability. To further confirm that THR conferred the cell sensitivity to paclitaxel, cell viability was assessed after treatment with paclitaxel and paclitaxel and THR (4 μ M). Values were presented as the percentage of cell survival relative to DMSO. Data were shown with the means \pm SD. (F and G) Total cell lysates from Aspc-1 (F), SW1990 (F), Panc-02 (G), and Panc-02-PTX (G) cell lines were obtained after cells were treated with paclitaxel in a dose-dependent manner. They were analyzed for the expressions of FoxM1 and PHB1. β -actin was used as a loading control. (H) The mRNA was detected in the cell lysates in Aspc-1 and SW1990 cells. (I) The mRNA was detected in Panc-02 and Panc-02-PTX cells. One-way ANOVA post Tukey's multiple comparison test was used for statistical analysis. * $p < 0.05$, ** $p < 0.01$, *** $p < 0.001$.

inherent resistance? We found that overexpression of FoxM1b or FoxM1c conferred Panc-02 resistance to paclitaxel, as indicated by the increase in IC_{50} compared with the control. Depletion of PHB1 in Panc-02 attenuated the paclitaxel resistance induced by FoxM1. Moreover, THR increased the sensitivity of Panc-02 to paclitaxel (Figure 5E). The protein and mRNA levels of FoxM1 and PHB1 were observed in Aspc-1, SW1990, Panc-02, and Panc-02-PTX cells, which indicated that FoxM1 and PHB1 were stable in paclitaxel-resistant cell lines when treated with paclitaxel (Figures 5F–5I). Targeting FoxM1 and PHB1 may provide a strategy to reverse paclitaxel resistance.

ABCA2 Promoted the Paclitaxel Efflux and Was Regulated by the FoxM1/PHB1/RAF-MEK-ERK Pathway

Depletion of PHB1 in the paclitaxel-resistant SW1990 cell line significantly increased drug efflux (Figure S6A). Drug efflux was controlled by the elevated level of ABC transporters, which consisted of 7 subfamilies.³³ Moreover, as P-gp (ABCB1) had been excluded from the mechanism of FoxM1-induced paclitaxel resistance (Figures S1F and S1G), we deduced that increased drug efflux might be driven by the elevated expression of other ABC transporters. HEK293T cells were transfected with FoxM1b, FoxM1c, FoxM1b + H1, and FoxM1c + H1, which

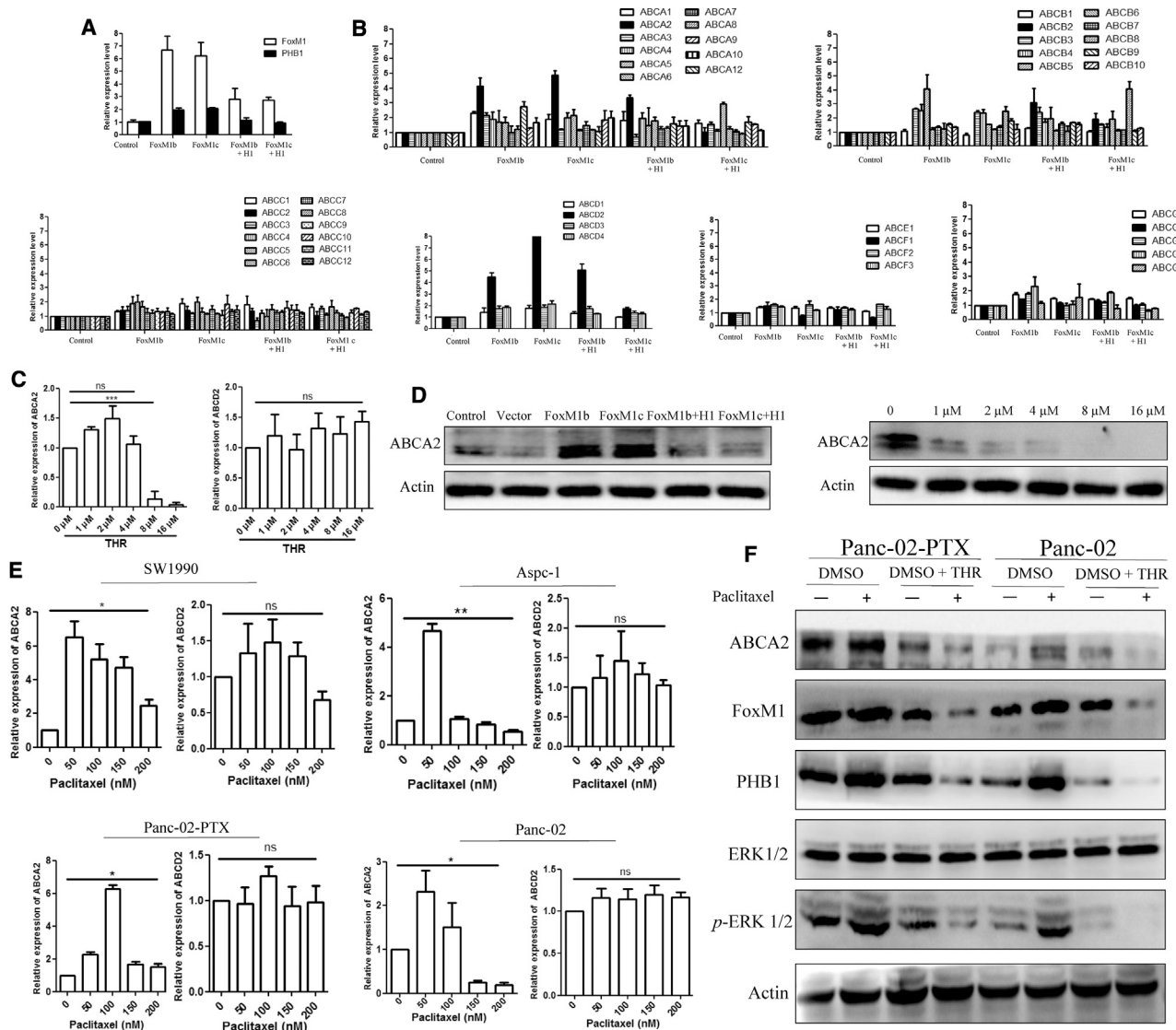


Figure 6. The Expressions of ABCA2 Transporters Was under the Regulation of the FoxM1/PHB1/RAF-MEK-ERK Pathway in HEK293T Cells

(A) HEK293T cells were transfected with penter-FoxM1b, penter-FoxM1c, penter-FoxM1b and H1, and penter-FoxM1c and H1. FoxM1 and PHB1 mRNA levels were analyzed by qRT-PCR. Data were represented as means \pm SD. (B) mRNA levels of ABC transporters were detected in 47 cases. Specific oligonucleotide probes are listed in Table S2. 7 subtypes of ABC are displayed in (A). (C) THR decreased the ABCA2 mRNA level but had no effect on ABCD2 in HEK293T. Statistical analysis was performed by one-way ANOVA post hoc Tukey test. *** $p < 0.001$. (D) ABCA2 was under the regulation of FoxM1. Overexpression of FoxM1b or FoxM1c increased the ABCA2 protein level, while knockdown of PHB1 rescued the upregulation of ABCA2. Suppression of FoxM1 by THR in a dose-dependent manner significantly decreased the ABCA2. All the experiments were performed in HEK293T cells. (E) ABCA2 and ABCD2 were analyzed by qRT-PCR after 24-h paclitaxel treatment. The expressions of ABC transporters were determined in Aspc-1, SW1990, Panc-02, and Panc-02-PTX cells. One-way ANOVA post Tukey's multiple comparison test was used for statistical analysis. * $p < 0.05$, ** $p < 0.01$, *** $p < 0.001$. (F) The expressions of ABCA2, FoxM1, PHB1, ERK1/2, and p-ERK1/2 were analyzed in the cells treated with DMSO, 10 nM paclitaxel, 4 μ M THR, 10 nM paclitaxel, and 4 μ M THR.

significantly altered the mRNA levels of FoxM1 and PHB1 (Figure 6A).

We profiled the mRNA levels of 47 human ABC transporters to screen which ABC transporter contributed to paclitaxel resistance under the regulation of the FoxM1/PHB1/RAF-MEK-ERK pathway. Among these ABC transporter molecules, the mRNA of ABCA2 and

ABCD2 were significantly upregulated in HEK293T cells when transfected with FoxM1b or FoxM1c. Adversely, PHB1 depletion significantly decreased the mRNA levels of ABCA2 and ABCD2 (Figure 6B). ABCD2 was not affected when it was treated with an increasing dose of THR (Figure 6C). We found an increase of ABCA2 in HEK293T cells when transfected with FoxM1b or FoxM1c; but, the effect was attenuated when we knocked down the PHB1. THR also sharply

inhibited the expression of ABCA2 (Figure 6D). Moreover, SW1990, Panc-02, and Panc-02-PTX treated with paclitaxel had elevated mRNA of ABCA2, but not ABCD2 (Figure 6E). Further study confirmed that, when cells were treated with paclitaxel and THR, the mRNA levels of FoxM1, PHB1, and ABCA2 were significantly declined, while ABCD2 was not (Figure S5A). We concluded that ABCA2 was regulated by the FoxM1/PHB1/RAF-MEK-ERK-signaling pathway and promoted paclitaxel resistance.

Afterward, the protein levels were also detected. Panc-02-PTX and Panc-02 cells treated with paclitaxel and/or THR showed that ABCA2, FoxM1, PHB1, and *p*-ERK1/2 were increased when confronted with paclitaxel at 10 nM, but they were significantly decreased when combined with THR (Figure 6F). Similar results were confirmed in SW1990 and Aspc-1 (Figure S5B). The difference was that FoxM1, PHB1, *p*-ERK1/2, and ABCA2 were not increased in Aspc-1 when treated with paclitaxel at the concentration of 10 nM. In summary, overexpressing FoxM1b or FoxM1c induced the increase in PHB1 in the cell membrane and enhanced the binding of PHB1 to C-RAF, which led to paclitaxel resistance by activating the RAF/MEK/ERK pathway. Moreover, ABCA2 also sustained the drug efflux under the regulation of the FoxM1/PHB1/RAF-MEK-ERK feedback loop.

Pancreatic Cancer Paclitaxel-Resistant Cells Treated with Paclitaxel Displayed Cellular Apoptosis following THR Treatment or PHB1 Depletion

SW1990 cells treated with THR significantly increased paclitaxel influx. Cells stained with Oregon Green 488 paclitaxel exhibited cellular apoptosis morphology of nucleation, which was indicated by arrows (Figure 7A). The quantification was performed by flow cytometry (Figure 7B). Besides, depletion of PHB1 in SW1990 induced the cells to be more sensitive to paclitaxel (Figure S6A). To confirm that FoxM1b or FoxM1c increased PHB1 to promote paclitaxel drug resistance, Panc-02 cells were transfected with FoxM1b or FoxM1c, which conferred the cell resistance to Oregon Green 488 paclitaxel, while knocking down PHB1 could attenuate the effect (Figure 7C). The result was consistent with Figure 5E. Our analysis is presented in Figure 7D. These clearly indicate that depletion of PHB1 by FoxM1 induced the cellular apoptosis and the sensitivity to paclitaxel.

We attempted to assess the efficacy of THR in a paclitaxel-resistant model *in vivo*. Cells treated with THR significantly decreased the proliferation, migration, and invasion (Figure S2). Here, Panc-02-PTX cells were used to establish the orthotopic tumor model in C57BL/6 mice. Panc-02-PTX cells displayed a wide range of cancer metastases (Figure S8A). Panc-02-PTX treated with paclitaxel and THR showed a significant reduction in the tumor growth, while paclitaxel treatment alone had a slight effect (Figure S7A). The combination of paclitaxel and THR prolonged the survival time (Figure 7E). Consistently, the combined therapy significantly reduced tumor volume and weight in a subcutaneous xenograft model (Figures 7F and 7H; Figure S8B). In addition, it was well tolerated in mice with no obvious weight

changes observed (Figure 7G). Our *in vivo* results indicated that THR could reverse the drug resistance and improve the paclitaxel efficiency.

The Expressions of FoxM1, PHB1, and ABCA2 in Human Pancreatic Cancer Tumors and Their Association with the Features of Clinical Drug Resistance

We detected the correlations between FoxM1 and PHB1 in 56 tumor tissues from pancreatic cancer patients. Immunofluorescent analysis demonstrated that FoxM1 and PHB1 were located in the cytoplasm and nuclei (Figure 8A). We also found that, in the same tumor tissue, the higher FoxM1 expression was positively correlated with the levels of PHB1, ABCA2, and *p*-ERK1/2 (Figure 8B; Figure S9A). Because the clinical information for the sensitivity to the chemotherapeutic drugs was unavailable, fresh tumor was obtained and minced into smaller fragments (1 mm³) immediately after the surgery. Pancreatic primary cancer cells were collected after being resuspended in digestive enzyme reagent and incubated in the incubator. The patients were divided into paclitaxel-sensitive and -resistant groups. Cells with an average fluorescent intensity less than 60% were considered to be resistant to Oregon Green 488 paclitaxel (100 nM); otherwise they were considered to be sensitive to paclitaxel (sensitive, n = 21; resistant, n = 35).

The mRNA was detected in the adjacent normal tissue and tumor among the sensitive and resistant patients. The expression levels of FoxM1, PHB1, and ABCA2 were higher in the tumors of resistant patients than in those of sensitive ones. Besides, there was no difference between adjacent normal tissue and tumor in the sensitive patients (Figure S9B). Univariate and multivariate Cox-regression analyses were used to evaluate FoxM1, PHB1, and ABCA2 expression patterns and the clinicopathological parameters. FoxM1, PHB1, and ABCA2 overexpressions were associated with a higher risk of death in univariate analysis. The same results were obtained after we adjusted tumor stage and lymph node involvement (Table S1). We found a positive correlation between the expressions of FoxM1 and PHB1, FoxM1 and *p*-ERK1/2, and FoxM1 and ABCA2 in the sensitive and resistant groups. FoxM1 and survival time were negatively correlated (Figure 8B). To confirm that FoxM1-induced PHB1 and ABCA2 expressions were dependent on ERK signaling, we incubated the primary cell lines, which were resistant to paclitaxel, with the ERK1/2 inhibitor SCH772984 (SCH). SCH could partially suppress ABCA2, FoxM1, PHB1, and *p*-ERK1/2 protein expressions. Paclitaxel and SCH in combination sharply decreased the protein abundance (Figure 8C). These data further supported the notion that FoxM1 positively regulated PHB1 and ABCA2 via activating the RAF-MEK-ERK pathway to promote paclitaxel resistance.

DISCUSSION

In this research, we explored the critical roles of FoxM1 in the drug resistance of pancreatic cancer cells and the underlying mechanisms. We found that FoxM1b and FoxM1c directly activated the transcription of PHB1, constituting a novel signaling pathway that conferred the pancreatic cancer cell resistance to paclitaxel. Our mechanistic

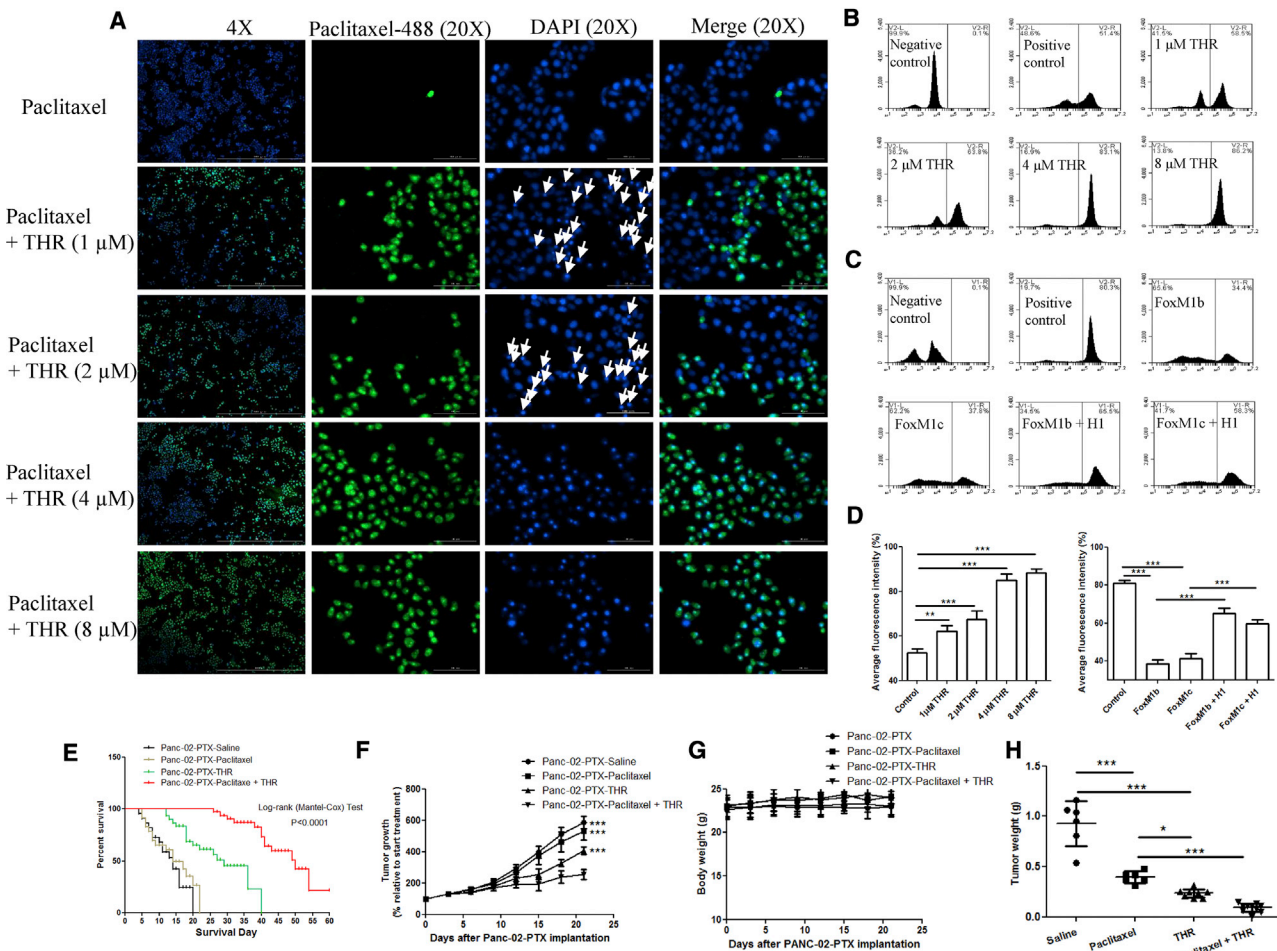


Figure 7. In Vitro and In Vivo Cytotoxicity Study Revealed that the FoxM1/PHB1/RAF-MEK-ERK Pathway Affected Paclitaxel Chemotherapeutic Efficacy

(A) SW1990 cells were treated with THR at the dosages of 1, 2, 4, and 8 μ M, respectively. 24 h after incubation with THR, 100 nM Oregon Green 488 paclitaxel was incubated for 12 h additionally. Cells were fixed and counterstained with DAPI (blue) and visualized by the Cytation 5 Cell Imaging Multi-Mode Reader (BioTek). Paclitaxel-targeted cells are indicated by arrows. Scale bar, 100 μ m. (B) FACS was used to analyze the average fluorescent intensity of Oregon Green 488 paclitaxel (100 nM) after treatment with THR (1, 2, 4, and 8 μ M) in SW1990. Cells untreated and treated with Oregon Green 488 paclitaxel (100 nM) were used as negative and positive controls, respectively. (C) FACS was used to analyze the average fluorescent intensity of Oregon Green 488 paclitaxel in Panc-02 cells that were transfected with FoxM1b, FoxM1c, FoxM1b + H1, and FoxM1c + H1. Cells untreated and transfected with vector were used as negative and positive controls, respectively. (D) Quantification of Oregon Green 488 paclitaxel-positive cells after treatment with THR or plasmid transfection by flow cytometric analysis. Experiments were repeated four times. One-way ANOVA post Tukey's multiple comparison test was used for statistical analysis. * $p < 0.05$, ** $p < 0.01$, *** $p < 0.001$. (E) Kaplan-Meier survival was analyzed in the tumor-bearing mice ($n = 16$ per group). The survival time was set from 2 weeks after the Panc-02-PTX (1×10^6) cells were inoculated in the pancreas. Log rank test was used to compare the difference between different groups. *** $p < 0.0001$. (F) C57BL/6 mice were inoculated subcutaneously with 1×10^6 Panc-02-PTX cells. The animals were divided randomly into four groups. When the average tumor volume within each group was at least 50–120 mm^3 , saline ($n = 6$), paclitaxel (10 mg/kg, $n = 6$), THR (80 mg/kg, $n = 8$), paclitaxel (10 mg/kg), and THR (80 mg/kg, $n = 10$) were administered at the indicated time points. Tumor growth was determined on the day of treatment relative to the start of treatment and presented as a percentage. Data were compared with the last time of drug treatment among the four groups. (G) The actual body weights of the four groups are shown during the drug treatment. (H) The resected tumor weight at the end of the treatment. Each curve represents the average tumor growth \pm SD of at least six mice per group. One-way ANOVA post Tukey's multiple comparison test was used for statistical analysis. The data were compared with the saline group. * $p < 0.05$, ** $p < 0.01$, *** $p < 0.001$.

and clinical evidence strongly suggested that deregulated FoxM1 caused abnormal PHB1 expression and critically contributed to pancreatic cancer pathogenesis and paclitaxel resistance.

Multiple factors contributed to paclitaxel resistance within a given cell population, and these factors were highly variable. Mechanisms of

resistance included the alterations of tubulin, signal transduction pathways, and/or oncogene activation.⁵ Previous research had proven that FoxM1 conferred the paclitaxel resistance by regulating KIF20A or ABCC5,^{34,35} which drove the abnormal formation of mitotic spindle or drug efflux. Besides, FoxM1 regulated microtubule dynamics via targeting tubulin-destabilizing protein stathmin to protect

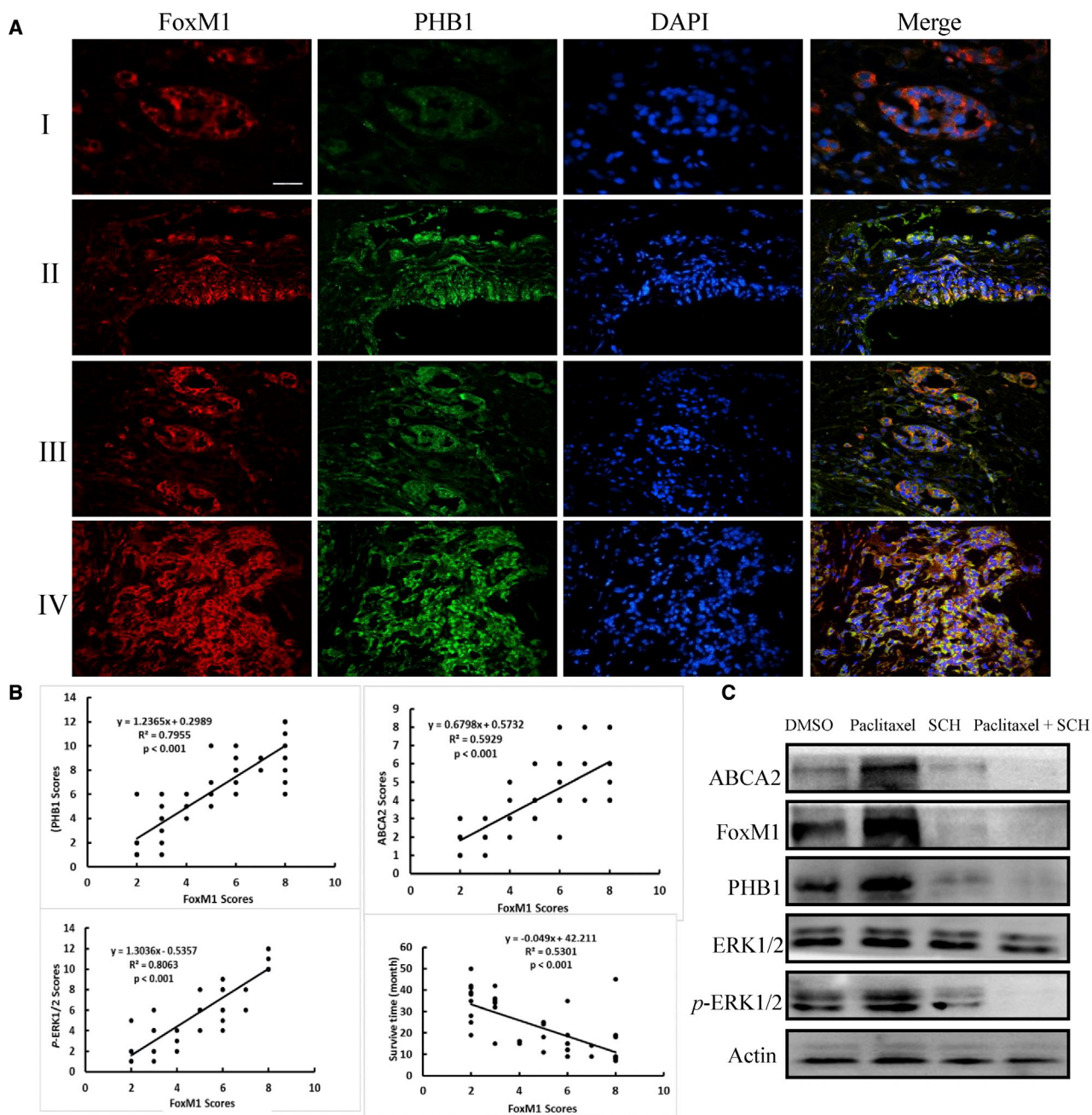


Figure 8. FoxM1 and PHB1 Overexpression Is Significantly Associated with Poorer Survival in Pancreatic Cancer Patients

(A) Immunofluorescent staining was used to analyze the expressions of FoxM1 and PHB1 in pancreatic patients. It showed that the expressions of FoxM1 and PHB1 were significantly associated with clinical stage. (B) FoxM1, PHB1, ABCA2, and p-ERK1/2 expressions in human pancreatic tumors and normal pancreatic tissue were measured by the standard immunohistochemical procedures with specific antibodies. The staining results were scored by 2 investigators blinded to the clinical data. Correlations between the levels of FoxM1 and PHB1, FoxM1 and ABCA2, FoxM1 and p-ERK1/2, and FoxM1 and survival time were observed in the pancreatic cancer tissue and patients. FoxM1 expression correlated inversely with survival time, but it positively correlated with PHB1, ABCA2, and p-ERK1/2 expressions. Pearson correlation analysis was used for statistical analysis. * $p < 0.05$, ** $p < 0.01$, *** $p < 0.001$. Note: some of the dots on the graphs represented more than one specimen (overlapped scores). (C) Immunoblotting was used to analyze the expressions of ABCA2, FoxM1, PHB1, ERK1/2, and p-ERK1/2 in primary pancreatic cancer cells (resistant to paclitaxel), which were treated with DMSO, 10 nM paclitaxel, 4 nM SCH, 10 nM paclitaxel, and 4 nM SCH, respectively.

the tumor cell from paclitaxel-induced apoptosis.¹⁰ FoxM1 transcriptionally activated the Cav-1 gene, constituting a novel signaling pathway that directly impacted invasion and metastasis of pancreatic cancer cells.¹³ SPFH domain-containing proteins were special lipid rafts.³⁶ Roles of the SPFH superfamily in carcinogenesis had been studied extensively. Proteins of this superfamily, such as flotillins and stomatins, shared common features with caveolins. The GeneMANIA network was assigned to identify whether there was an interaction between FoxM1 and PHB1. They were co-expressed in the cells and clustered in the GEO data from Ramaswamy et al.²⁵ Moreover, we demonstrated that FoxM1 positively regulated the expression of PHB1 at the transcriptional level through a Forkhead response element (FHRE). Besides, FoxM1 enhanced PHB1 stabilization and activated a feedback circuit to promote paclitaxel resistance.

The expression of PHB1 was decreased in the sensitive pancreatic cancer cells and deregulated in the paclitaxel-resistant cells when they were treated with paclitaxel. FoxM1b and FoxM1c conferred the cells' resistance to paclitaxel by regulating PHB1 and activating the MAPK-signaling pathway. Numerous studies had examined the expression level of PHB1 in paclitaxel-resistant cell lines and drew different conclusions.^{18,37,38} Cicchillitti et al.³⁷ indicated that PHB1 was significantly elevated in cell lysates in paclitaxel-resistant cell lines when compared with its sensitive counterpart, whereas Patel et al.³⁸ showed that there was no difference between the paclitaxel-sensitive and -resistant cell lines, but it was elevated in membrane fractions in paclitaxel-resistant cell lines. In our study, we detected that PHB1 expression level was positively correlated with the capability of resistance in pancreatic cancer cells and non-small-cell lung cancer cells. It was elevated in plasma membrane fractions in paclitaxel-resistant cells compared with parental cells. Meanwhile, PHB1 and FoxM1 were affected when confronted with paclitaxel in sensitive and resistant cell lines. Both were decreased in the whole-cell lysate in Aspc-1, but not reduced significantly in SW1990. Similar results were obtained in the Panc-02 and Panc-02-PTX cells. So, we concluded that FoxM1 and PHB1 were involved in the molecular mechanism of paclitaxel resistance.

There were 3 isoforms of FoxM1 protein owing to the different splicing of exons. FoxM1b and FoxM1c functioned as transcriptional activators, whereas FoxM1a was transcriptionally inactive.^{9,39} FoxM1b and FoxM1c promoted the proliferation, migration, and metastasis of pancreatic cancer cells. FoxM1b showed a potent regulatory effect on PHB1 compared with FoxM1c, which might be due to fact that the transactivation domain was completely inhibited by the auto-inhibitory N terminus of FoxM1c.⁹ FoxM1b or FoxM1c conferred Aspc-1 resistance to paclitaxel. As expected, depletion of PHB1 abolished the drug resistance, which was induced by FoxM1b or FoxM1c. FoxM1b or FoxM1c mediated the translocation of PHB1 from the nucleus to the plasma membrane, which enhanced the interaction between PHB1 and C-RAF and contributed to an increase in the phosphorylation of ERK1/2 in the MAPK-signaling pathway. Indeed, Rajalingam et al.¹² showed that PHB1 was necessary for the recruitment of C-RAF to caveolin-1-rich lipid rafts and activation of the RAS-RAF-MEK-ERK pathway.

Interestingly, we also found that the depletion of PHB1 induced a decrease in *p*-ERK1/2 and FoxM1. Previous studies had confirmed that FoxM1 was regulated by the activity of ERK1/2. Suppression of FoxM1 decreased the phosphorylation of ERK1/2 and induced massive apoptosis in human cancer cell lines.^{40,41} Therefore, we concluded that FoxM1/PHB1/RAF-MEK-ERK had formed a positive feedback loop to increase the cell proliferation, migration, invasion, and drug resistance. One of the signaling pathways that was activated in response to microtubule disruption was ERK1/2.^{5,42-44} FoxM1 was one of the major ERK1/2 effectors, whose overexpression occurred in various experimental and human tumors.^{32,40} Indeed, FoxM1 triggered the degradation of ERK1/2 inhibitor DUSP1 via the transcriptional activation of SKP2 and CKS1, and thus it reinforced the ERK1/2 activity in human cancer cells. Further study should demonstrate if the activations of FoxM1/SKP2-CKS1 and FoxM1/PHB1 that governed the interaction between paclitaxel resistance and ERK1/2 activity were additive, synergistic, or antagonistic.

Paclitaxel-resistant cells harbored a higher level of mitochondrial membrane potential, which was sensitive to Rho123. However, the reverse relationship between paclitaxel resistance and Rho123 resistance was evaluated (Figures S1H and S1I), which was similar to the relationship between *cis*-Diamminedichloroplatinum (DDP) and Rho123.²¹ THR decreased Rho123 retention and increased the intracellular concentration of paclitaxel in the drug-resistant cell lines. To eliminate the possibility that the decrease in Rho123 retention by THR was due to an increase in ABCB1,²⁵ we tested the 4 cell lines for cross-resistance to DOX.²¹ In a clonogenic assay, we found that Aspc-1, SW1990, Panc-02, and Panc-02-PTX cells had virtually identical values of IC₅₀ as DOX. PHB1 was essential for mitochondrial integrity and membrane potential.^{18,19} THR decreased the membrane potential and inhibited the level of PHB1 and ABCA2 simultaneously, which accelerated the influx of Oregon Green 488 paclitaxel into the drug-resistant cell and induced cellular apoptosis.

Hou et al.³⁵ analyzed the correlations between FoxM1 and ABC transporters by depleting FoxM1, which significantly lowered the mRNA levels of ABCA2 and ABCC5. They excluded ABCA2 was regulated by FoxM1 because there was no difference between the expression level of ABCA2 in CNE2TR and CNE2 cells, which had different FoxM1 protein levels. However, in our study, HEK293T transfected with FoxM1b or FoxM1c increased the expression of ABCA2, whereas ABCC5 was not affected. Overexpression of FoxM1 and depletion of PHB1 simultaneously reduced the protein and mRNA levels of ABCA2. In summary, ABCA2 was regulated by the FoxM1/PHB1/RAF-MEK-ERK pathway and participated in the paclitaxel resistance.

Besides, treating cells with paclitaxel at the dosage of 10 nM showed that FoxM1, PHB1, ABCA2, and *p*-ERK1/2 were upregulated in the SW1990, Panc-02, and Panc-02-PTX cells, but not the Aspc-1 cells. By comparing with the expression levels at higher concentrations of paclitaxel, we concluded that the expression levels of FoxM1, PHB1, ABCA2, and *p*-ERK1/2 were also associated with drug dosage.

It was confirmed that paclitaxel-induced ERK1/2 activation was related to the levels of ERK1/2 activity,⁴⁴ suggesting that, in tumors with higher ERK1/2 activity, there may be an application for this strategy in therapy. The combination of THR and paclitaxel significantly decreased the protein abundance and sensitized the paclitaxel-resistant cells.

In conclusion, we clearly demonstrated the function of FoxM1 and PHB1 in the maintenance of resistance to paclitaxel in human pancreatic cancer cells. Silencing either or both of the molecules rendered cells sensitive to paclitaxel both *in vitro* and *in vivo*. As FoxM1 was a potent modulator that conferred drug resistance via different signaling pathways, we did not propose that FoxM1/PHB1/RAF-MEK-ERK was the only pathway that contributed to paclitaxel resistance. However, drugs that specifically targeted the FoxM1, such as THR, may bring hope to paclitaxel treatment.

MATERIALS AND METHODS

Cell Culture and Treatment

Aspc-1, Bxpc-3, Panc-01, Panc-02, SW1990, H1650, HCC827, H1975, A549, and HEK293T cell lines were obtained from Type Culture Collection of Chinese Academy of Sciences (Shanghai, China). Paclitaxel (Cytoskeleton, TXD01, Denver, CO, USA) or SCH772984 (Target Molecule, T6066, Boston, MA, USA) was dissolved in DMSO and added to the media at the indicated concentrations and time points. THR (Tocris Bioscience, 3267, MO, USA) was dissolved in DMSO or oil and protected from light. For transient transfection and drug treatment, all the cell confluence was 60%–80%. Penter-FoxM1b, Penter-FoxM1c, and PHB1-Penter were purchased from Vigene Bio (CH811655, CH825506, and CH862869, Rockville, MD, USA). LentiCRISPRv2 was a gift from Dr. Huapeng Li in the Department of Molecular, Cell and Cancer Biology, University of Massachusetts Medical School. The sgRNAs (single guide RNAs) targeting the coding sequence of the human PHB1 gene are listed in [Table S2](#). Plentiv2-PHB1 (H1, H2, and H3) with the different sgRNAs was constructed and sequenced. GenJet Plus *in vitro* DNA Transfection Reagent (SignaGen Laboratories, SL100499, Rockville, MD, USA) was used for transfection. Overexpressing and silencing effects were successfully verified by western blot.

Generation of Drug-Resistant Cell Lines to Paclitaxel

When Panc-02 or A549 cells were at 70%–80% confluence, paclitaxel was added to the medium at the $IC_{50}/5$ determined previously. We removed the media after 48 h. Within approximately 1–2 weeks, resistant clones appeared evidently under the microscope. When cells were at about 70%–80% confluence, we added $2 \times IC_{50}/5$ concentration of paclitaxel again and then got the resistant clones. In a similar method, a dose-escalation concentration of paclitaxel was added to generate a stable population of cells in flasks under the highest concentration. The dose-escalation protocol could be implemented for up to 4 months until the $2 \mu\text{M}$ concentration was reached. The cells were named after Panc-02-PTX or A549-PTX, respectively.

The Analysis of Cell Membrane Potential

Panc-02, Panc-02-PTX, A549, and A549-PTX cell lines were treated with DMSO, paclitaxel, paclitaxel, and THR respectively for 24 h. Then we changed to fresh medium and incubated with Rho123 ($5 \mu\text{g}/\text{mL}$) for 15 min. After that, cell pellets were collected. The FL1 channel was used to detect the cell membrane potential, which was indicated by the average fluorescent intensity of Rho123.

Western Blotting and CoIP

Cells and tumor samples were homogenized (Bertin Precellys Evolution) in ice-cold lysis buffer. Lysates were centrifuged at $8,000 \times g$ at 4°C for 10 min. The supernatant protein concentration was detected by a protein assay kit (Bio-Rad, Hercules, CA, USA). Proteins were separated by 10% SDS-PAGE and transferred onto Immobilon-P^{SQ} polyvinylidene fluoride (PVDF) $0.2\text{-}\mu\text{m}$ membranes (Millipore). Antibodies were purchased as follows: FoxM1 (Cell Signaling Technology, 5436, Danvers, MA, USA), PHB1 (Abcam, ab28172, MA), C-RAF (Cell Signaling Technology, 9421), phospho-ERK1/2 (Cell Signaling Technology, 4370), ERK1/2 (Cell Signaling Technology, 9102), ABCA2 (Novus Biologicals, NBP1-20863, Littleton, CO, USA), and β -actin (Sigma-Aldrich, A2103, Shanghai, China). For each immunoprecipitation (coIP), cell lysates were incubated with $0.5 \mu\text{g}$ of the indicated antibody at 4°C with rotation overnight. $30 \mu\text{L}$ Protein G Agarose Beads was added (Cell Signaling Technology, 37478) to the cell lysates and then incubated at 4°C for 4 h. We centrifuged for 5 min at 16,000 rpm, then removed the supernatant. Agarose Beads were then washed with 1 mL cold PBS three times. The precipitates were resuspended by $60 \mu\text{L}$ SDS loading buffer, and subsequent analysis was performed as the procedure described above.

Cell and Tissue Immunofluorescence

Panc-02 and Panc-02-PTX cells were fixed with 4% paraformaldehyde after treatment or transfection at the indicated time points. Then we permeabilized the cells with 0.1% Triton100. After that cells were immersed three times in Tris-buffered saline (TBS) and incubated with the PHB1 primary antibody (sc-28259, diluted 1:200; Santa Cruz Biotechnology, TX) overnight at 4°C and the corresponding Cy3 goat anti-rabbit secondary antibodies (3101, diluted 1:150; Earthox, Millbrae, CA, USA) for 1 h at room temperature (RT). DAPI (diluted 1:1,000; Sigma-Aldrich) was used to stain the nucleus. Tissue sections were performed on a microtome (HM 430, MICROM International, Walldorf, Germany). Sections were blocked with 5% BSA in PBS for 30 min and incubated with the primary mouse monoclonal antibody anti-FoxM1 (sc-271746, diluted 1:100; Santa Cruz Biotechnology) or polyclonal rabbit antibody against PHB1 (sc-28259, diluted 1:200; Santa Cruz Biotechnology), respectively, at 4°C overnight. The primary antibodies were detected with the secondary antibodies (sheep anti-mouse or goat anti-rabbit). After immunolabeling, the tissue samples were incubated with $1 \mu\text{g}/\text{mL}$ DAPI and covered in 0.1% 1, 4-diazabicyclo [2.2.2] octane (DABCO; Sigma-Aldrich). Microscopic images of cells were obtained using an Olympus IX71.

Flow Cytometric Analysis

For the detection of PHB1, cells were collected after transfection with FoxM1b, FoxM1c, vector, and THR (4 μ M and 8 μ M). Cells were washed with cold TBS twice, and then rinsed in 0.1% Triton100 in TBS or 0.5% Triton100 in TBS 3 times, respectively. They were incubated with PHB1 antibody (Santa Cruz Biotechnology, sc-28259) for 60 min at RT and then with Cy3 goat anti-rabbit IgG for 60 min at RT. After being rinsed in TBS three times, cells were immediately subjected to the flow cytometry analysis. Samples were detected on a BD C6 (BD Pharmingen) and data were analyzed with FlowJo software, version 10.1.

Chromatin Immunoprecipitation Assay

ChIP was performed according to the standard protocol from the Cell Signaling Technology Chromatin IP Kit (9004S). Briefly, the cell was cross-linked with 37% formaldehyde (final concentration was 1%) at RT. 0.5 μ L Micrococcal Nuclease was used to digest DNA to a length of approximately 150–200 bp. 500 μ L diluted chromatin was transferred to a 1.5-mL micro-tube; a 10- μ L sample of the diluted chromatin was picked out as a 2% input sample. The ChIP-Grade FoxM1 antibody (GeneTex, GTX102170) was added to the 5 μ g diluted, digested, and cross-linked chromatin. For the positive control, 10 μ L Histone H3 (Rabbit mAb 4620) was added to the IP sample. For the negative control, 1 μ L Rabbit IgG 2729 was added to the IP sample (except 2% input sample) with rotation overnight at 4°C. 30 μ L ChIP-Grade Protein G Agarose Beads was added to each IP reaction (except 2% input sample), and then we incubated them for 2 h at 4°C with rotation. We eluted chromatin from the antibody and protein G Agarose Beads at 65°C for 30 min with gentle vortex, and we reversed the cross-linked and 2% input sample by adding 6 μ L 5 M NaCl and 2 μ L Proteinase K to it for 2 h at 65°C. All the samples were purified by spin columns. 2 μ L DNA sample was used for each ChIP-qPCR amplification. Results were presented as the relative enrichment to input sample. Data were compared to IgG and Histone H3 treatments. All primers used in ChIP-qPCR assays are listed in [Table S2](#).

Orthotopic and Subcutaneous Tumor Cell Implantation

C57BL/6 mice (42–56 days) were purchased from the Experimental Animals Center of Tongji Medical College, Huazhong University of Science and Technology. To establish an orthotopic pancreatic cancer model, mice were anesthetized with pentobarbital sodium. A small flank incision of the left abdomen was made and the spleen was exteriorized. 1×10^6 Panc-02-PTX cells were injected subcapsularly in a region of the pancreas as described previously.⁴⁵ The survival analysis of tumor-bearing mice was conducted after 2 weeks of the surgical operation. For the paclitaxel-resistant tumor model, 1×10^6 cells were inoculated at the flank region of C57BL/6 mice subcutaneously. When the tumor volume reached 50–100 mm³, tumor-bearing mice were weighed and divided into four groups ($n = 6$ in Panc-02-PTX model for saline treatment, $n = 6$ in Panc-02-PTX model for paclitaxel treatment, $n = 8$ in Panc-02-PTX model for THR treatment, and $n = 10$ in Panc-02-PTX model for paclitaxel and THR treatment). Paclitaxel and THR were injected into the lateral tail vein of

C57BL/6 mice at 3-day intervals, 4 times, at doses of paclitaxel 10 mg/kg and THR 80 mg/kg (THR was administered 4 h after paclitaxel). During this period, the body weight and tumor size were monitored every 3 days. After the last treatment, the mice were sacrificed. Tumors were weighed and main organs were collected. All the procedures were approved by the Committee of Animal Care of Huazhong University of Science and Technology.

Tumor Tissue Collection and Analysis

We obtained pancreatic cancer tissues from patients who had undergone pancreatic resections. All the sample diagnoses were confirmed by histopathology; we received the informed consent from all subjects and the identification from committee that approved the studies. Tissues were fixed in paraformaldehyde solution for 24 h and subsequently paraffin embedded for histological analysis. Cells digested from fresh samples were resuspended in cell culture for the detection of drug sensitivity ([Supplemental Materials and Methods](#)). The mRNA was extracted with Trizol reagent. The detailed clinical and pathological data were obtained from each patient. Patients who survived less than 2 months after surgery were excluded from the survival analysis in order to rule out surgery-related mortality.⁴⁶ The study was approved by the local Ethics Committee, and written informed consent was obtained from patients prior to surgery.

Statistical Analysis

The results were presented as the mean \pm SE. One-way ANOVA followed by Tukey's post hoc test and the Student's *t* test was used to evaluate statistical significance. Statistical analyses were performed using SPSS 22.0 software, GraphPad Prism 5.0, and Windows Excel. Categorical variables were compared using chi-square tests or Fisher exact tests. The correlations among the protein levels were assessed by bi-variate Pearson correlation analysis. Patients' survival was estimated by Kaplan-Meier estimation and compared by log rank test. The univariate and multivariate analyses were carried out by Cox-regression model. Statistical differences were considered to be significant when $p < 0.05$.

SUPPLEMENTAL INFORMATION

Supplemental Information can be found online at <https://doi.org/10.1016/j.omto.2019.05.005>.

AUTHOR CONTRIBUTIONS

C.H. conceived the experiments and M.X. secured funding. C.H., X.Z., L.J., and L.Z. performed the experiments and analyzed the data. C.H. and X.Z. wrote the manuscript. H.R. edited and approved the manuscript.

CONFLICTS OF INTEREST

The authors declare no competing interests.

ACKNOWLEDGMENTS

The authors thank Dr. Huapeng Li from the Department of Molecular, Cell and Cancer Biology, University of Massachusetts Medical School for providing lentiCRISPRv2 and technical assistance.

REFERENCES

- Galletti, E., Magnani, M., Renzulli, M.L., and Botta, M. (2007). Paclitaxel and docetaxel resistance: molecular mechanisms and development of new generation taxanes. *ChemMedChem* 2, 920–942.
- Robey, R.W., Pluchino, K.M., Hall, M.D., Fojo, A.T., Bates, S.E., and Gottesman, M.M. (2018). Revisiting the role of ABC transporters in multidrug-resistant cancer. *Nat. Rev. Cancer* 18, 452–464.
- Dumontet, C., and Sikic, B.I. (1999). Mechanisms of action of and resistance to anti-tubulin agents: microtubule dynamics, drug transport, and cell death. *J. Clin. Oncol.* 17, 1061–1070.
- Drukman, S., and Kavallaris, M. (2002). Microtubule alterations and resistance to tubulin-binding agents (review). *Int. J. Oncol.* 21, 621–628.
- Orr, G.A., Verdier-Pinard, P., McDaid, H., and Horwitz, S.B. (2003). Mechanisms of Taxol resistance related to microtubules. *Oncogene* 22, 7280–7295.
- Raychaudhuri, P., and Park, H.J. (2011). FoxM1: a master regulator of tumor metastasis. *Cancer Res.* 71, 4329–4333.
- Priller, M., Pöschl, J., Abrão, L., von Bueren, A.O., Cho, Y.J., Rutkowski, S., Kretzschmar, H.A., and Schüller, U. (2011). Expression of FoxM1 is required for the proliferation of medulloblastoma cells and indicates worse survival of patients. *Clin. Cancer Res.* 17, 6791–6801.
- Kim, I.M., Ackerson, T., Ramakrishna, S., Tretiakova, M., Wang, I.C., Kalin, T.V., Major, M.L., Gusarova, G.A., Yoder, H.M., Costa, R.H., and Kalinichenko, V.V. (2006). The Forkhead Box m1 transcription factor stimulates the proliferation of tumor cells during development of lung cancer. *Cancer Res.* 66, 2153–2161.
- Kong, X., Li, L., Li, Z., Le, X., Huang, C., Jia, Z., Cui, J., Huang, S., Wang, L., and Xie, K. (2013). Dysregulated expression of FOXM1 isoforms drives progression of pancreatic cancer. *Cancer Res.* 73, 3987–3996.
- Carr, J.R., Park, H.J., Wang, Z., Kiefer, M.M., and Raychaudhuri, P. (2010). FoxM1 mediates resistance to herceptin and paclitaxel. *Cancer Res.* 70, 5054–5063.
- Katoh, M., Igarashi, M., Fukuda, H., Nakagama, H., and Katoh, M. (2013). Cancer genetics and genomics of human FOX family genes. *Cancer Lett.* 328, 198–206.
- Rajalingam, K., Wunder, C., Brinkmann, V., Churin, Y., Hekman, M., Sievers, C., Rapp, U.R., and Rudel, T. (2005). Prohibitin is required for Ras-induced Raf-MEK-ERK activation and epithelial cell migration. *Nat. Cell Biol.* 7, 837–843.
- Huang, C., Qiu, Z., Wang, L., Peng, Z., Jia, Z., Logsdon, C.D., Le, X., Wei, D., Huang, S., and Xie, K. (2012). A novel FoxM1-caveolin signaling pathway promotes pancreatic cancer invasion and metastasis. *Cancer Res.* 72, 655–665.
- Head, B.P., Patel, H.H., Roth, D.M., Murray, F., Swaney, J.S., Niesman, I.R., Farquhar, M.G., and Insel, P.A. (2006). Microtubules and actin microfilaments regulate lipid raft/caveolae localization of adenylyl cyclase signaling components. *J. Biol. Chem.* 281, 26391–26399.
- Bickel, P.E., Scherer, P.E., Schnitzer, J.E., Oh, P., Lisanti, M.P., and Lodish, H.F. (1997). Flotillin and epidermal surface antigen define a new family of caveolae-associated integral membrane proteins. *J. Biol. Chem.* 272, 13793–13802.
- Wang, S., Fusaro, G., Padmanabhan, J., and Chellappan, S.P. (2002). Prohibitin co-localizes with Rb in the nucleus and recruits N-CoR and HDAC1 for transcriptional repression. *Oncogene* 21, 8388–8396.
- Wang, S., Zhang, B., and Faller, D.V. (2002). Prohibitin requires Brg-1 and Brm for the repression of E2F and cell growth. *EMBO J.* 21, 3019–3028.
- Gregory-Bass, R.C., Olatinwo, M., Xu, W., Matthews, R., Stiles, J.K., Thomas, K., Liu, D., Tsang, B., and Thompson, W.E. (2008). Prohibitin silencing reverses stabilization of mitochondrial integrity and chemoresistance in ovarian cancer cells by increasing their sensitivity to apoptosis. *Int. J. Cancer* 122, 1923–1930.
- Chowdhury, I., Xu, W., Stiles, J.K., Zeleznik, A., Yao, X., Matthews, R., Thomas, K., and Thompson, W.E. (2007). Apoptosis of rat granulosa cells after staurosporine and serum withdrawal is suppressed by adenovirus-directed overexpression of prohibitin. *Endocrinology* 148, 206–217.
- Baracca, A., Sgarbi, G., Solaini, G., and Lenaz, G. (2003). Rhodamine 123 as a probe of mitochondrial membrane potential: evaluation of proton flux through F₀ during ATP synthesis. *Biochim. Biophys. Acta* 1606, 137–146.
- Zinkewich-Péotti, K., and Andrews, P.A. (1992). Loss of cis-diamminedichloroplatinum(II) resistance in human ovarian carcinoma cells selected for rhodamine 123 resistance. *Cancer Res.* 52, 1902–1906.
- Tapiero, H., Munck, J.N., Fourcade, A., and Lampidis, T.J. (1984). Cross-resistance to rhodamine 123 in Adriamycin- and daunorubicin-resistant Friend leukemia cell variants. *Cancer Res.* 44, 5544–5549.
- Deuchars, K.L., Du, R.P., Naik, M., Evernden-Porelle, D., Kartner, N., van der Blik, A.M., and Ling, V. (1987). Expression of hamster P-glycoprotein and multidrug resistance in DNA-mediated transformants of mouse LTA cells. *Mol. Cell. Biol.* 7, 718–724.
- Coates, P.J., Nenutil, R., McGregor, A., Picksley, S.M., Crouch, D.H., Hall, P.A., and Wright, E.G. (2001). Mammalian prohibitin proteins respond to mitochondrial stress and decrease during cellular senescence. *Exp. Cell Res.* 265, 262–273.
- Ramaswamy, S., Tamayo, P., Rifkin, R., Mukherjee, S., Yeang, C.H., Angelo, M., Ladd, C., Reich, M., Latulippe, E., Mesirov, J.P., et al. (2001). Multiclass cancer diagnosis using tumor gene expression signatures. *Proc. Natl. Acad. Sci. USA* 98, 15149–15154.
- Pei, H., Li, L., Fridley, B.L., Jenkins, G.D., Kalari, K.R., Lingle, W., Petersen, G., Lou, Z., and Wang, L. (2009). FKBP51 affects cancer cell response to chemotherapy by negatively regulating Akt. *Cancer Cell* 16, 259–266.
- Littler, D.R., Alvarez-Fernández, M., Stein, A., Hibbert, R.G., Heidebrecht, T., Aloy, P., Medema, R.H., and Perrakis, A. (2010). Structure of the FoxM1 DNA-recognition domain bound to a promoter sequence. *Nucleic Acids Res.* 38, 4527–4538.
- Wierstra, I., and Alves, J. (2006). Despite its strong transactivation domain, transcription factor FOXM1c is kept almost inactive by two different inhibitory domains. *Biol. Chem.* 387, 963–976.
- Dai, B., Kang, S.H., Gong, W., Liu, M., Aldape, K.D., Sawaya, R., and Huang, S. (2007). Aberrant FoxM1B expression increases matrix metalloproteinase-2 transcription and enhances the invasion of glioma cells. *Oncogene* 26, 6212–6219.
- Zhang, Y., Zhang, N., Dai, B., Liu, M., Sawaya, R., Xie, K., and Huang, S. (2008). FoxM1B transcriptionally regulates vascular endothelial growth factor expression and promotes the angiogenesis and growth of glioma cells. *Cancer Res.* 68, 8733–8742.
- Rajalingam, K., and Rudel, T. (2005). Ras-Raf signaling needs prohibitin. *Cell Cycle* 4, 1503–1505.
- Calvisi, D.F., Pinna, F., Meloni, F., Ladu, S., Pellegrino, R., Sini, M., Daino, L., Simile, M.M., De Miglio, M.R., Virdis, P., et al. (2008). Dual-specificity phosphatase 1 ubiquitination in extracellular signal-regulated kinase-mediated control of growth in human hepatocellular carcinoma. *Cancer Res.* 68, 4192–4200.
- Zhang, J.T. (2007). Use of arrays to investigate the contribution of ATP-binding cassette transporters to drug resistance in cancer chemotherapy and prediction of chemosensitivity. *Cell Res.* 17, 311–323.
- Khongkow, P., Gomes, A.R., Gong, C., Man, E.P., Tsang, J.W., Zhao, F., Monteiro, L.J., Coombes, R.C., Medema, R.H., Khoo, U.S., and Lam, E.W. (2016). Paclitaxel targets FOXM1 to regulate KIF20A in mitotic catastrophe and breast cancer paclitaxel resistance. *Oncogene* 35, 990–1002.
- Hou, Y., Zhu, Q., Li, Z., Peng, Y., Yu, X., Yuan, B., Liu, Y., Liu, Y., Yin, L., Peng, Y., et al. (2017). The FOXM1-ABCC5 axis contributes to paclitaxel resistance in nasopharyngeal carcinoma cells. *Cell Death Dis.* 8, e2659.
- Browman, D.T., Hoegg, M.B., and Robbins, S.M. (2007). The SPFH domain-containing proteins: more than lipid raft markers. *Trends Cell Biol.* 17, 394–402.
- Cicchillitti, L., Di Michele, M., Urbani, A., Ferlini, C., Donat, M.B., Scambia, G., and Rutilio, D. (2009). Comparative proteomic analysis of paclitaxel sensitive A2780 epithelial ovarian cancer cell line and its resistant counterpart A2780TC1 by 2D-DIGE: the role of ERp57. *J. Proteome Res.* 8, 1902–1912.
- Patel, N., Chatterjee, S.K., Vrbanc, V., Chung, I., Mu, C.J., Olsen, R.R., Waghorne, C., and Zetter, B.R. (2010). Rescue of paclitaxel sensitivity by repression of Prohibitin1 in drug-resistant cancer cells. *Proc. Natl. Acad. Sci. USA* 107, 2503–2508.
- Laoukili, J., Stahl, M., and Medema, R.H. (2007). FoxM1: at the crossroads of ageing and cancer. *Biochim. Biophys. Acta* 1775, 92–102.
- Yoshida, Y., Wang, I.C., Yoder, H.M., Davidson, N.O., and Costa, R.H. (2007). The forkhead box M1 transcription factor contributes to the development and growth of mouse colorectal cancer. *Gastroenterology* 132, 1420–1431.

41. Wierstra, I., and Alves, J. (2007). FOXM1, a typical proliferation-associated transcription factor. *Biol. Chem.* 388, 1257–1274.
42. Shinohara-Gotoh, Y., Nishida, E., Hoshi, M., and Sakai, H. (1991). Activation of microtubule-associated protein kinase by microtubule disruption in quiescent rat 3Y1 cells. *Exp. Cell Res.* 193, 161–166.
43. Schmid-Alliana, A., Menou, L., Manié, S., Schmid-Antomarchi, H., Millet, M.A., Giuriato, S., Ferrua, B., and Rossi, B. (1998). Microtubule integrity regulates src-like and extracellular signal-regulated kinase activities in human pro-monocytic cells. Importance for interleukin-1 production. *J. Biol. Chem.* 273, 3394–3400.
44. McDaid, H.M., and Horwitz, S.B. (2001). Selective potentiation of paclitaxel (taxol)-induced cell death by mitogen-activated protein kinase kinase inhibition in human cancer cell lines. *Mol. Pharmacol.* 60, 290–301.
45. Bruns, C.J., Harbison, M.T., Kuniyasu, H., Eue, I., and Fidler, I.J. (1999). In vivo selection and characterization of metastatic variants from human pancreatic adenocarcinoma by using orthotopic implantation in nude mice. *Neoplasia* 1, 50–62.
46. Varghese, F., Bukhari, A.B., Malhotra, R., and De, A. (2014). IHC Profiler: an open source plugin for the quantitative evaluation and automated scoring of immunohistochemistry images of human tissue samples. *PLoS ONE* 9, e96801.